CHAPTER 4

RESULTS AND DISCUSSIONS

4.1 Introduction

The previous chapter established analytical formulations for various non-polynomial shear deformation theories. These theories are based on advanced trigonometric functions, including the "secant function" i.e. Trigonometric Shear Deformation Theory (TSDT) and the "inverse hyperbolic sine function" i.e. Inverse Hyperbolic Shear Deformation Theory (IHSDT). These formulations are critical as they provide the mathematical foundation needed to analyze the static, buckling and free vibration responses of carbon nanotube reinforced composite beam structures.

This chapter leverages these advanced formulations to explore three primary responses of the carbon nanotube reinforced composite beam with and without an elastic foundation:

- Static Response
- Buckling Response
- Free Vibration Response

The chapter develops an analytical model for carbon nanotube-reinforced composite beams, crucial for assessing their response to mechanical loads in structural engineering. The bending analysis of carbon nanotube-reinforced composite beams examines transverse deflection, normal stresses, in-plane shear stresses, and transverse shear stresses under mechanical loads, influenced by variations in key parameters. Furthermore, the effect of these parametric conditions is examined in the buckling analysis of the carbon nanotube reinforced composite beam under uniaxial compressive load. Following the bending analysis, the carbon nanotube reinforced composite beam is subjected to a free vibration analysis to determine its natural frequencies under different parametric conditions. Specifically, the analysis focuses on:

- The variation of the reinforcement distribution pattern of carbon nanotubes across the thickness of the carbon nanotube reinforced composite beam.
- The volume fraction of carbon nanotubes within the carbon nanotube reinforced composite beam.
- The length-to-thickness ratio of the beam.
- A range of other influencing factors.

Through this detailed analysis, the chapter provides comprehensive insights into the static, buckling and free vibration behaviors of carbon nanotube reinforced composite beams under various loading and parametric conditions.

In the final part of the chapter, the analytical modeling of a carbon nanotube reinforced composite beam resting on the Pasternak elastic foundation is utilized to determine the structural response under mechanical loads. This section covers the bending, free vibration, and buckling responses of the CNTRC beam resting on an elastic foundation. The bending analysis aims to understand the deformation of carbon nanotube reinforced composite beam resting on the Pasternak elastic foundation under mechanical loads, focusing on transverse deflection, normal stresses, in-plane shear stresses, and transverse shear stresses. The bending response is examined by varying these parameters to observe the transverse deflection and stress distribution change of the beam under mechanical loads.

Further, the free vibration analysis determines the natural frequencies of the carbon nanotube reinforced composite beam resting on the Pasternak elastic foundation when it vibrates without external forces after being disturbed. The analysis considers various parametric conditions to understand their effect on the dynamic behaviour of the beam.

Following the free vibration analysis, the buckling analysis focuses on the stability of the CNTRC beam resting on an elastic foundation under uniaxial compressive loads. It aims to identify the critical load at which the beam becomes unstable and buckles.

These responses are affected by changes to different parameters, primarily including:

- Reinforcement Distribution Pattern: The arrangement of carbon nanotubes across the thickness of carbon nanotube reinforced composite beam.
- Volume Fraction of Carbon Nanotubes: The proportion of carbon nanotubes in the carbon nanotube reinforced composite beam.
- Winkler Spring Constant Factor: This factor represents the stiffness of the elastic foundation in the vertical direction.
- Shear Layer Constant Factor: This factor accounts for the shear interaction between the beam and the elastic foundation.
- Length-to-Thickness Ratio: The ratio of the length to the thickness of the beam.

This detailed analysis aids in optimizing the design and composition of carbon nanotube reinforced composite beams for improved performance and reliability in practical applications.

Vibration analysis is vital in structural engineering for assessing structural conditions, detecting faults, and preventing failures. By measuring and interpreting vibration signals, engineers evaluate dynamic characteristics and predict behavior under various conditions. The two main types are free and forced vibration analysis.

Free vibration analysis examines a structure's natural frequencies by allowing it to vibrate without external forces. It is crucial for determining dynamic characteristics, predicting behavior, and ensuring structural integrity, particularly in critical components like turbine blades and pump impellers.

Free vibration analysis identifies a structure's natural frequencies, helping engineers design to avoid resonance and potential damage. It also aids in diagnosing structural issues by analyzing vibration signals to address problems before failures occur. Free vibration analysis predicts structural behavior under various conditions, ensuring safe and reliable designs. It is widely used in aerospace to assess aircraft and spacecraft integrity and in automotive engineering to evaluate components like suspensions and engine mounts.

The free vibration analysis of carbon nanotube-reinforced composite beams on a Pasternak elastic foundation examines natural frequencies under varying parameters, including CNT distribution, volume fraction, Winkler spring constant, shear layer constant, and length-to-thickness ratio. This analysis enhances the understanding of their dynamic behavior for improved design and reliability.

Buckling occurs when a structure, like a column or beam, becomes unstable under axial loads exceeding a critical value. This failure is due to buckling rather than the applied load itself and is influenced by factors such as material properties, geometry, and load nature.

Importance of Buckling Load Analysis:

- Evaluating Structural Integrity:

Buckling load analysis is crucial for assessing the strength and stability of structures, helping identify potential issues before failure and ensuring the integrity of critical components like columns, beams, and plates.

- Determining Critical Buckling Load:

Buckling load analysis helps determine the critical load at which a structure will buckle and fail, allowing engineers to design structures that avoid this load and prevent damage.

- Evaluating Strength Under Different Loads:

Buckling load analysis helps engineers assess how a structure will respond to different loads, enabling designs that ensure safe and reliable performance under various conditions.

- Diagnosing Structural Problems:

Analyzing the buckling behavior helps engineers diagnose the root causes of structural problems. For instance, if a column shows signs of buckling due to inadequate bracing, engineers can implement additional bracing to prevent further issues.

- Predicting Behavior Under Various Conditions:

The analysis is valuable for predicting how structures will behave under different operating conditions, such as varying loads, temperatures, or pressures. This prediction is crucial for designing structures that can perform safely and reliably in diverse environments.

The analysis of buckling loads in carbon nanotube reinforced composite beams resting on the Pasternak elastic foundation involves a detailed examination of how different parameters affect the critical buckling load. The critical buckling load is influenced by several factors:

- Reinforcement Distribution Pattern:

The variation in the distribution pattern of carbon nanotubes across the thickness of the carbon nanotube reinforced composite beam significantly affects its buckling behavior. Different distribution patterns can enhance or reduce the stability of the beam.

- Volume Fraction of Carbon Nanotubes:

The amount of carbon nanotubes within the carbon nanotube reinforced composite beam plays a crucial role in its overall strength and stability. Varying the volume fraction helps in optimizing the performance of the beam under axial loads.

- Winkler Spring Constant Factor:

This factor represents the stiffness of the foundation supporting the beam. Changes in the Winkler spring constant affect how the beam interacts with the foundation, influencing its buckling response.

- Shear Layer Constant Factor:

The shear layer constant factor accounts for the shear interactions within the foundation. Variations in this factor impact the stability of the beam and its susceptibility to buckling.

- Length-to-Thickness Ratio:

The ratio of the length to the thickness of the beam is a critical geometric parameter. Adjusting this ratio alters the buckling characteristics of the beam, with longer and thinner beams generally being more prone to buckling.

Analyzing these parameters provides insights into the buckling behavior of carbon nanotube reinforced composite beams, enabling the design of robust beams that withstand axial loads and ensure safe, effective performance.

Based on advanced theories and principles, mathematical models are derived to describe the behavior of carbon nanotube reinforced composite beams. These models account for various factors such as the distribution of carbon nanotubes, mechanical loads, and the characteristics of the foundation. These theories, using trigonometric functions like the secant function and the inverse hyperbolic sine function, provide the basis for the analytical formulations. The derived mathematical models are translated into MATLAB code. MATLAB is chosen for its powerful computational and visualization capabilities, making it suitable for implementing complex analytical formulations. The MATLAB code runs simulations to solve the mathematical models, producing numerical results for various structural responses of the beams, such as bending, free vibration, and buckling. The results obtained from the MATLAB simulations are validated by comparing them with existing results in the literature.

The chapter is organized into several sections and subsections, each addressing different structural analysis problems of carbon nanotube reinforced composite beams. The analysis begins with the structural examination of the beams, including bending, free vibration, and buckling analyses.

1. Bending Analysis:

This section investigates the bending behavior of the carbon nanotube reinforced composite beams under various loading and parametric conditions.

It includes assessments of transverse deflection, normal stresses, in-plane shear stresses, and transverse shear stresses.

2. Free Vibration Analysis:

Following the bending analysis, the chapter delves into the free vibration analysis of the carbon nanotube reinforced composite to determine their natural frequencies and vibration modes under different conditions.

3. Buckling Analysis:

This section examines the buckling behavior of the carbon nanotube reinforced composite under uniaxial loading conditions, evaluating their stability and critical buckling loads.

4. Analysis of the Pasternak Elastic Foundation:

The subsequent section explores the structural analysis of the carbon nanotube reinforced composite resting on the Pasternak elastic foundation. It covers bending, free vibration, and buckling analyses under this specific foundation model.

The final section of the chapter provides a summary and conclusions, bringing the analysis to a close.

4.2 Material characteristics

The continuous mathematical functions listed below are employed to characterize the distributions of material constituents. **Table 4.1** illustrates the relationship between reinforcement distribution and beam thickness, specifying the corresponding volume fractions of carbon nanotubes (CNTs) for the models indicated.

Table 4.1 Distribution relationship for the volume fraction of CNTRC beams

Distribution type	Distribution relationship
UD Beam	$V_{cnt} = V_{cnt}^{*}$
FG-V Beam	$V_{cnt} = (1 + \frac{2Z}{h})\, V_{cnt}^{*}$
FG-O Beam	$V_{cnt} = 2(1 - 2\frac{\lvert z \rvert}{h})\, V_{cnt}^{*}$
FG-X Beam	$V_{cnt} = 4\frac{\lvert z \rvert}{h} V_{cnt}^{*}$

In the above table, $"h"$ denotes the thickness of the beam, while $"z"$ stands for the reference value in that direction. The distribution of carbon nanotubes (CNTs) in the matrix changes the mechanical characteristics of the FG-CNTRC beam. The several CNT distribution approaches in the transverse direction of the beam are considered for the study under parametric circumstances. The use of Poly methyl methacrylate (PMMA) as the matrix material and armchair (10,10) as the reinforcement material in the research on composite beams is based on the fact that PMMA has a strong ability to bond and armchair (10,10) has a high impact resistance.

The FG-CNTRC beams used in this research currently have the following material characteristics at room temperature. Matrix made up of poly methyl methacrylate (PMMA) consists of subsequent material properties. $V^{p} = 0.3$; $\rho^{p} = 1190$ kg/m^3; and $E^{p} = 2.5$ Gpa. The SWCNTs utilized as an armchair (10, 10) for reinforcing comprise of $V_{cnt} = 0.19$; $\rho^{cnt} = 1400$ kg/m^3; $E_{11}^{cnt} = 600$ Gpa; $E_{22}^{cnt} = 10$ Gpa; and $G_{12}^{cnt} = 17.2$ Gpa. The bond strength of SWCNTs and PMMA, which serve as reinforcement and matrix for different CNT volume fractions, is determined using molecular dynamics simulations.

The volume fraction of the CNTs and their pattern of distribution as reinforcement affect the mechanical property of the FG-CNTRC beam. An efficiency parameter called 'η_i' is defined for various CNT volume fractions, and it has an impact on the mechanical properties of the FG-CNTRC beam. The efficiency parameter for CNTs η_I (I = 1, 2, 3), are proposed which are based on the properties of SWCNTs that depend on their size. In **Table 4.2**, the efficiency parameter values for various CNT volume fractions are listed.

Table 4.2 CNTs efficiency parameter

V_{cnt}^*	η_1	η_2	η_3
0.12	1.2833	1.0556	1.0556
0.17	1.3414	1.7101	1.7101
0.28	1.3238	1.7380	1.7380

4.3 Structural analysis of the composite beam reinforced with carbon nanotube

This section conducts a detailed structural analysis of carbon nanotube reinforced composite beams, covering bending analysis, free vibration analysis, and buckling analysis.

Bending Analysis

The bending analysis evaluates the beam response under various loading and parametric conditions. It includes examining:

- Transverse Deflection: The displacement perpendicular to the length of the beam due to applied loads.
- Normal Stresses: Stresses acting perpendicular to the cross-sectional area of the beam.
- In-plane Shear Stresses: Stresses parallel to the plane of the beam that arises within its material.
- Transverse Shear Stresses: Stresses that act across the thickness of the beam.

Free Vibration Analysis

Following the bending analysis, the free vibration analysis is performed to determine the natural frequencies of the composite beam. This analysis helps in understanding how the beam vibrates when it is not subjected to continuous external forces, providing insights into its dynamic behavior.

Buckling Analysis

Next, the buckling analysis is carried out under uniaxial loading conditions. This analysis identifies the critical load at which the beam becomes unstable and buckles, which is crucial for ensuring the structural integrity of the beam under compressive forces.

Material and Structural Configuration

For these analyses, a simply supported carbon nanotube reinforced composite beam is selected. The beam is composed of carbon nanotubes as the reinforcing fibers embedded in a PMMA (polymethyl methacrylate) matrix. The detailed material properties of the composite beam are provided in Chapter 3, specifically in Section 3.9.

4.3.1 Static analysis of carbon nanotube reinforced composite beams

In this section, the bending behavior of carbon nanotube reinforced composite beams is examined. The analysis includes evaluating transverse deflection, normal stresses, in-plane shear stresses, and transverse shear stresses under various parametric conditions. These conditions encompass:

- Variation in the reinforcement distribution pattern of carbon nanotubes across the thickness of carbon nanotube reinforced composite beams.
- The volume fraction of carbon nanotubes within the carbon nanotube reinforced composite beams beam.
- Length-to-thickness ratio of the beam.

The bending responses under these different parameters provide insights into how changes in the distribution and quantity of carbon nanotubes, as well as the geometry of the beam, affect its structural performance.

4.3.1.1. Dimensionless transverse displacement of CNT-Reinforced composite beams

The transverse deflection of a carbon nanotube reinforced composite beam under mechanical load is influenced by several parametric conditions. The distribution of carbon nanotubes (CNTs) across the thickness of the composite beam significantly affects its bending behavior. Different patterns, such as uniform distribution or gradation from one face to another, can change the stiffness and flexibility of the beam. For instance, concentrating CNTs near the surface may enhance surface stiffness but might reduce the overall flexibility.

The volume fraction, or the amount of CNTs present in the composite material, also plays a crucial role. A higher volume fraction of CNTs generally increases the stiffness and reduces deflection, as CNTs have higher mechanical strength compared to the matrix material. Conversely, a lower volume fraction would result in higher deflection under the same load due to less reinforcement. The ratio of the length to the thickness of the beam is a geometric parameter that influences its bending response. A higher length-to-thickness ratio typically means the beam is slender and more prone to bending under load, leading to greater deflection. A lower ratio indicates a thicker, more robust beam that deflects less under the same load.

4.3.1.1.1 Dimensionless transverse displacement of CNT-Reinforced composite beams under uniformly distributed load

Table 4.3 presents the variations in transverse deflection of a carbon nanotube reinforced composite beam under uniformly distributed load, considering different parameters such as the distribution pattern of carbon nanotube reinforcements across the thickness, volume fraction of carbon nanotubes, and span-to-thickness ratio. The data presented in the table is obtained through an analytical approach that utilizes trigonometric shear deformation theory, specifically employing the secant and inverse sine functions. The non-dimensional parameter for calculating the dimensionless transverse displacements of a simply supported CNTRC beam is given by $\overline{w} = \frac{E_p w 10^{3}}{q_0 L^4}\left(\frac{L}{2}\right)$.

The table shows that the transverse deflection of the carbon nanotube reinforced composite beam under uniformly distributed load varies similarly to the span thickness ratio when other factors are held constant. This suggests that as the span thickness ratio increases, the transverse deflection decreases, assuming all other factors remain unchanged. When other factors are constrained, increasing the volume fraction of CNTs in the carbon nanotube reinforced composite beam leads to a decrease in the non-dimensional transverse deflection.

This implies that higher concentrations of CNTs contribute to increased stiffness and reduced deflection under transverse loading. For a specific volume fraction of CNTs and span thickness ratio, different reinforcement distribution patterns (FG-X, UD, FG-V, FG-O) exhibit varying levels of resistance to transverse deflection. The FG-X distribution shows the minimum deflection, while the FG-O distribution exhibits the maximum deflection. This suggests that the arrangement of CNTs within the composite structure plays a significant role in determining its mechanical behavior under transverse loading. Among the considered reinforcement distribution patterns, FG-X offers the highest resistance to transverse deflection, followed by UD, FG-V, and FG-O. This indicates that certain distribution patterns, such as FG-X, provide better mechanical properties in terms of resisting deflection under transverse loading. Similarly, the stiffness of the carbon nanotube reinforced composite beam follows a descending order among the reinforcement distribution patterns, with FG-X being the stiffest and FG-O being the least stiff. This highlights the influence of reinforcement distribution on the overall stiffness and mechanical behavior of the composite structure. The current findings are compared with those of Karamanli and Vo (2012), and

Wattanasakulpong and Ungbhakorn (2013) which present results from shear and normal deformation theory (SNDT) and third-order beam theory (TBT) respectively. These comparisons demonstrate a strong alignment between the outcomes obtained in this study and those reported in the referenced studies.

Table 4.3 Non-dimensional transverse displacements of carbon nanotube reinforced composite beam subjected to uniformly distributed load

V^*_{CNT}	*L/h*	Theory	UD	FG-O	FG-X	FG-V
	5	**Present (IHSDT)**	1.6350	2.2791	1.4583	1.8227
		Present (TSDT)	1.6388	2.2736	1.5521	1.9017
		Karamanli and Vo (2021)	1.6443	2.1637	1.4964	1.8177
	10	**Present (IHSDT)**	0.7369	1.1837	0.5935	0.9259
		Present (TSDT)	0.7482	1.1754	0.6085	0.9370
		Karamanli and Vo (2021)	0.7038	1.0977	0.5767	0.8783
0.12	15	**Present (IHSDT)**	0.5588	0.9735	0.4202	0.7481
		Present (TSDT)	0.5630	0.9692	0.4260	0.7522
		Karamanli and Vo (2021)	0.5240	0.8978	0.3995	0.6990
	20	**Present (IHSDT)**	0.4955	0.8994	0.3584	0.6849
		Present (TSDT)	0.4977	0.8968	0.3616	0.6871
		Wattanasakulpong and Ungbhakorn (2013)	0.4610	-	-	-
	5	**Present (IHSDT)**	1.0030	1.3914	0.9042	1.1327
		Present (TSDT)	1.0463	1.3899	0.9524	1.1746
		Karamanli and Vo (2021)	1.0022	1.3210	0.9178	1.1221
	10	**Present (IHSDT)**	0.4710	0.7666	0.3786	0.6026
		Present (TSDT)	0.4774	0.7631	0.3859	0.6086
0.17		**Karamanli and Vo (2021)**	0.4490	0.7128	0.3661	0.5711
	15	**Present (IHSDT)**	0.3665	0.6475	0.2742	0.4984
		Present (TSDT)	0.3689	0.6457	0.2770	0.5007
		Karamanli and Vo (2021)	0.3438	0.5990	0.2603	0.4663
	20	**Present (IHSDT)**	0.3294	0.6056	0.2371	0.4615
		Present (TSDT)	0.3307	0.6045	0.2386	0.4627

		Wattanasakulpong and Ungbhakorn (2013)	0.3070	-	-	-
	5	**Present (IHSDT)**	0.7813	0.9878	0.7504	0.8581
		Present (TSDT)	0.7919	0.9931	0.7912	0.8979
		Karamanli and Vo (2021)	0.7951	0.9569	0.7667	0.8630
	10	**Present (IHSDT)**	0.3369	0.5102	0.2893	0.4188
		Present (TSDT)	0.3429	0.5112	0.2932	0.4237
		Karamanli and Vo (2021)	0.3250	0.4798	0.2806	0.4005
0.28	15	**Present (IHSDT)**	0.2476	0.4186	0.1948	0.3307
		Present (TSDT)	0.2498	0.4188	0.1959	0.3324
		Karamanli and Vo (2021)	0.2346	0.3903	0.1860	0.3117
	20	**Present (IHSDT)**	0.2158	0.3863	0.1609	0.2993
		Present (TSDT)	0.2170	0.3864	0.1614	0.3001
		Wattanasakulpong and Ungbhakorn (2013)	0.2030	-	-	-

4.3.1.1.2 Dimensionless transverse displacement of CNT-Reinforced composite beams under sinusoidal load

The analysis of the transverse deflection of a carbon nanotube (CNT) reinforced composite beam under a sinusoidal load is presented in **Table 4.4.** The analysis is based on an analytical solution using trigonometric shear deformation theory, specifically utilizing secant and inverse sine functions. The non-dimensional parameter for calculating the dimensionless transverse displacements of a simply supported CNTRC beam is given by $\overline{w} = \frac{E_p w 100 h^3}{q_0 L^4}\left(\frac{L}{2}\right)$.

The results from this analysis are compared with those obtained by Wattanasakulpong and Ungbhakorn (2013), showing a strong correlation and validation of the current findings. The table indicates that the transverse deflection of the carbon nanotube reinforced composite beam under sinusoidal load varies dissimilarly to the span thickness ratio when all other factors are held constant. This means that as the span thickness ratio increases, the transverse deflection decreases, assuming other variables remain unchanged. When other factors are constrained, increasing the volume fraction of CNTs in the carbon nanotube reinforced composite beam results in a decrease in the non-dimensional transverse deflection. This suggests that a higher CNT concentration enhances the stiffness of the composite, thereby reducing deflection under transverse loads. For a given volume fraction of CNTs and span thickness ratio, the non-dimensional transverse deflection varies depending on the CNT distribution pattern. The FG-X distribution pattern shows the minimum deflection, indicating the highest resistance to transverse loads, while the FG-O distribution exhibits the maximum deflection. The resistance to transverse deflection for a specific volume fraction of CNTs and span thickness ratio follows the order: FG-X, UD, FG-V, FG-O. This means FG-X offers the greatest resistance to deflection, followed by uniformly distributed (UD), FG-V, and finally FG-O distributions.

Table 4.4 Non-dimensional transverse displacements of carbon nanotube reinforced composite beam subjected to sinusoidal load

V^*_{CNT}	*L/h*	Theory	UD	FG-O	FG-X	FG-V
0.12	10	**Present (IHSDT)**	0.578	0.929	0.466	0.727
		Present (TSDT)	0.587	0.923	0.477	0.735
		Wattanasakulpong and Ungbhakorn (2013)	0.562	-	-	-
	15	**Present (IHSDT)**	0.438	0.766	0.330	0.587
		Present (TSDT)	0.442	0.761	0.334	0.590
		Wattanasakulpong and Ungbhakorn (2013)	0.416	-	-	-
	20	**Present (IHSDT)**	0.389	0.706	0.281	0.537
		Present (TSDT)	0.390	0.704	0.284	0.539
		Wattanasakulpong and Ungbhakorn (2013)	0.365	-	-	-
0.17	10	**Present (IHSDT)**	0.369	0.602	0.297	0.473

		Present (TSDT)	0.374	0.600	0.303	0.478
		Wattanasakulpong and Ungbhakorn (2013)	0.358	-	-	-
	15	**Present (IHSDT)**	0.287	0.508	0.215	0.391
		Present (TSDT)	0.289	0.507	0.217	0.393
		Wattanasakulpong and Ungbhakorn (2013)	0.273	-	-	-
	20	**Present (IHSDT)**	0.258	0.475	0.186	0.362
		Present (TSDT)	0.259	0.474	0.187	0.363
		Wattanasakulpong and Ungbhakorn (2013)	0.243	-	-	-
	10	**Present (IHSDT)**	0.264	0.400	0.227	0.328
		Present (TSDT)	0.269	0.401	0.230	0.332
		Wattanasakulpong and Ungbhakorn (2013)	0.260	-	-	-
	15	**Present (IHSDT)**	0.194	0.328	0.153	0.259
0.28		**Present (TSDT)**	0.196	0.328	0.153	0.261
		Wattanasakulpong and Ungbhakorn (2013)	0.187	-	-	-
	20	**Present (IHSDT)**	0.169	0.303	0.126	0.235
		Present (TSDT)	0.170	0.303	0.126	0.235
		Wattanasakulpong and Ungbhakorn (2013)	0.161	-	-	-

4.3.1.2 Dimensionless displacement and stress of CNT-Reinforced composite beams under sinusoidal load

The structural response of Uniformly Distributed (UD) beams subjected to sinusoidal loading is a critical topic in engineering research. Sinusoidal loads, characterized by their wave-like patterns, are common in various engineering applications and can significantly impact beam performance. This section presents a detailed analysis of the dimensionless displacements and stresses of UD carbon nanotube reinforced composite (CNTRC) beams under sinusoidal loading conditions. The analysis employs different theoretical models to understand how these beams behave under such loads, considering variations in span-to-thickness ratios (*L/h*) and CNT volume fractions (V_{cnt}^*). To facilitate a comprehensive and generalized comparison, the displacements and stresses are presented in dimensionless forms. Dimensionless analysis involves normalizing the actual measurements by dividing them by specific reference values, thereby eliminating unit-specific dependencies. This approach ensures that the results can be compared across different studies and scenarios without the limitations imposed by varying units of measurement. The non-dimensional parameter for calculating the dimensionless displacements and stress of a simply supported CNTRC beam is given by $\bar{w} = \frac{E_p w 100 h^3}{q_0 L^4}\left(\frac{L}{2}\right)$, $\bar{u} = \frac{E_p u 100 h^3}{q_0 L^4}(0, \frac{L}{2})$, $\bar{\sigma}_{xx} = \frac{h}{q_0 L}\sigma_{xx}(\frac{L}{2}, \frac{h}{2})$, $\bar{\sigma}_{xz} = \frac{h}{q_0 L}\sigma_{xz}(0,0)$.

In the table, the results are presented for the analytical solution using trigonometric shear deformation theory based on the secant and inverse sine function and compared with the results obtained by Wattanasakulpong and Ungbhakorn (2013) using Third-order Shear Deformation Theory (TSDT).

The table also displays the dimensionless deflection and stresses for the UD beam subjected to sinusoidal loads, calculated using trigonometric shear deformation theory, which is based on secant (TSDT) and inverse sine functions (IHSDT). The data are organized in tables that summarize the dimensionless displacements and stresses for different span-to-thickness ratios (*L/h*) and CNT volume fractions (V_{cnt}^*). Each row corresponds to a specific *L/h* ratio, a key parameter influencing the response of the beam. The span-to-thickness ratio is defined as the length of the beam (*L*) divided by its thickness (*h*), affecting the stiffness of the beam and consequently its deflection and stress distribution. **Tables 4.5** present the dimensionless displacements and stresses of UD beams for V_{cnt}^* = 0.12, 0.17, 0.28 respectively. Form the table it is observed that As the length-to-thickness ratio (*L/h*) increases, the dimensionless transverse displacement ($\bar{w}$) tends to decrease. This suggests that beams with higher *L/h* ratios (longer and thinner beams) exhibit less transverse deflection under sinusoidal loading. The dimensionless axial stress ($\bar{\sigma}_{xx}$) increases with higher *L/h* ratios, indicating greater internal forces within the material for longer beams. Increasing the CNT volume fraction V_{cnt}^{*} results in a decrease in dimensionless displacements, indicating enhanced stiffness and reduced deflection of the beams. The axial displacement ($\bar{u}$) also shows a decreasing trend with higher CNT content, reflecting the improved load-carrying capacity of the composite material.

Table 4.5 Non-dimensional displacements and stresses of UD beams under sinusoidal loading conditions

V^{*}_{CNT}	*L/h*	Theory	$\bar{w}$	$\bar{u}$	$\bar{\sigma}_{xx}$	$\bar{\sigma}_{xz}$
0.12	10	**Present (IHSDT)**	0.578	0.122	7.06	-
		Present (TSDT)	0.587	0.126	6.899	0.472
		Wattanasakulpong and Ungbhakorn (2013)	0.562	0.121	6.97	0.472
	15	**Present (IHSDT)**	0.438	0.055	9.78	-
		Present (TSDT)	0.442	0.056	9.668	0.475
		Wattanasakulpong and Ungbhakorn (2013)	0.41	0.054	9.716	0.475
	20	**Present (IHSDT)**	0.389	0.034	12.656	-
		Present (TSDT)	0.39	0.035	12.571	0.476
		Wattanasakulpong and Ungbhakorn (2013)	0.365	0.033	12.608	0.476
0.17	10	**Present (IHSDT)**	0.369	0.077	6.923	-
		Present (TSDT)	0.374	0.079	6.784	0.473
		Wattanasakulpong and Ungbhakorn (2013)	0.358	0.076	6.842	0.473
	15	**Present (IHSDT)**	0.287	0.035	9.687	-
		Present (TSDT)	0.289	0.036	9.591	0.475
		Wattanasakulpong and Ungbhakorn (2013)	0.273	0.035	9.63	0.475

	20	**Present (IHSDT)**	0.258	0.022	12.586	-
		Present (TSDT)	0.259	0.022	12.513	0.476
		Wattanasakulpong and Ungbhakorn (2013)	0.243	0.022	12.543	0.476
0.28	10	**Present (IHSDT)**	0.264	0.057	7.245	-
		Present (TSDT)	0.269	0.06	7.056	0.472
		Wattanasakulpong and Ungbhakorn (2013)	0.26	0.058	7.13	0.472
	15	**Present (IHSDT)**	0.194	0.025	9.906	-
		Present (TSDT)	0.196	0.026	9.774	0.475
		Wattanasakulpong and Ungbhakorn (2013)	0.187	0.025	9.824	0.475
	20	**Present (IHSDT)**	0.169	0.015	12.752	-
		Present (TSDT)	0.17	0.015	12.651	0.476
		Wattanasakulpong and Ungbhakorn (2013)	0.161	0.015	12.689	0.476

4.3.1.3 Dimensionless displacement and stress of CNT-Reinforced composite beams under uniformly distributed load

The investigation into the response of UD beams to uniformly distributed loading uncovered significant insights. Uniformly Distributed Load (UDL) loading patterns can significantly affect the performance of beams. UDL loading refers to a load distribution where the magnitude of the load is constant along the length of the beam. The analysis, particularly focusing on UD carbon nanotube reinforced composite (CNTRC) beams, sheds light on the deformation and stress patterns under UDL loading conditions. By employing trigonometric shear deformation theory based on the secant and inverse sine function and varying length-to-thickness ratios (L/h) and CNT volume fractions (V_{cnt}^{*}) we obtained valuable understanding. The non-dimensional parameter for calculating the dimensionless displacements and stress of a simply supported CNTRC beam is given by $\bar{w} = \frac{E_p w 100 h^3}{q_0 L^4}\left(\frac{L}{2}\right)$, $\bar{u} = \frac{E_p u 100 h^3}{q_0 L^4}(0, \frac{L}{2})$, $\bar{\sigma}_{xx} = \frac{h}{q_0 L}\, \sigma_{xx}(\frac{L}{2}, \frac{h}{2})$, $\bar{\sigma}_{xz} = \frac{h}{q_0 L}\sigma_{xz}(0,0)$.

Table 4.6 presents a comprehensive analysis of the dimensionless transverse deflection and stress of carbon nanotube reinforced composite (CNTRC) beams under a uniformly distributed load (UDL) condition. The table is significant as it offers a comparative study between the present results obtained from the trigonometric shear deformation theory based on the secant and inverse sine function and those from Third order Shear Deformation Theory (TSDT) by Wattanasakulpong and Ungbhakorn (2013). The comparison with Wattanasakulpong and Ungbhakorn (2013) provides a benchmark for validating the present research findings.

The table is structured to show the effects of varying the CNT volume fraction (V_{cnt}^*) and the length-to-thickness ratio (*L/h*) of the beam on the dimensionless transverse deflection ($\bar{w}$) and stress (σ). The CNT volume fractions considered are 0.12, 0.17, and 0.28, while the length-to-thickness ratios are 10, 15, and 20. These parameters are crucial in understanding the mechanical behavior of CNTRC beams, as they influence the stiffness and strength of the material. It is observed from the table as the CNT volume fraction increases, there is a general trend of increased stiffness, which is reflected in the reduced transverse deflection ($\bar{w}$). This is expected since a higher volume fraction of CNTs would enhance the composite's load-carrying capacity and resistance to deformation. This was further emphasized by the decreasing trend in axial displacement ($\bar{u}$) with higher CNT content, signifying the improved load-carrying capacity of the composite material. The table also shows that as the length-to-thickness ratio increases, the transverse deflection increases. This is in line with the principles of mechanics, where longer and thinner beams are more flexible and prone to bending under load. The stress values (σ) in the table indicate the distribution of stresses within the beam.

The variation in stress with different CNT volume fractions and length-to-thickness ratios can provide insights into the load-sharing mechanism between the CNTs and the matrix material. As the *L/h* ratio increases, the dimensionless axial stress ($\bar{\sigma}_{xx}$) also increases, signifying increased internal forces within the material for longer beams. Table also serves as a valuable resource for researchers and engineers working with CNTRC beams. It provides a systematic way to analyze the effects of CNT volume fraction and beam geometry on the mechanical response of the composite material under UDL conditions.

Table 4.6 Non-dimensional displacements and stresses of UD beams under uniformly distributed loading (UDL) conditions

V^*_{CNT}	*L/h*	Theory	$\bar{w}$	$\bar{u}$	$\bar{\sigma}_{xx}$	$\bar{\sigma}_{xz}$
0.12	10	**Present (IHSDT)**	0.737	0.156	7.576	0.680
		Present (TSDT)	0.741	0.161	7.012	0.700
		Wattanasakulpong and Ungbhakorn (2013)	0.704	0.173	8.399	0.701
	15	**Present (IHSDT)**	0.559	0.071	11.500	0.688
		Present (TSDT)	0.563	0.072	11.429	0.709
		Wattanasakulpong and Ungbhakorn (2013)	0.524	0.074	11.849	0.716
	20	**Present (IHSDT)**	0.496	0.044	15.397	0.690
		Present (TSDT)	0.497	0.046	15.421	0.719
		Wattanasakulpong and Ungbhakorn (2013)	0.461	0.045	15.448	0.725
0.17	10	**Present (IHSDT)**	0.471	0.098	7.599	0.682
		Present (TSDT)	0.477	0.100	7.492	0.702
		Wattanasakulpong and Ungbhakorn (2013)	0.449	0.107	8.268	0.704
	15	**Present (IHSDT)**	0.367	0.045	11.516	0.689
		Present (TSDT)	0.368	0.046	11.486	0.691
		Wattanasakulpong and Ungbhakorn (2013)	0.344	0.048	11.762	0.719
	20	**Present (IHSDT)**	0.329	0.029	15.092	0.691

		Present (TSDT)	0.333	0.029	15.012	0.709
		Wattanasakulpong and Ungbhakorn	0.307	0.029	15.384	0.726
	10	**Present (IHSDT)**	0.337	0.073	7.545	0.678
		Present (TSDT)	0.342	0.075	7.490	0.681
		Wattanasakulpong and Ungbhakorn (2013)	0.325	0.082	8.562	0.697
	15	**Present (IHSDT)**	0.248	0.032	11.479	0.686
0.28		**Present (TSDT)**	0.249	0.032	11.318	0.710
		Wattanasakulpong and Ungbhakorn (2013)	0.235	0.034	11.959	0.714
	20	**Present (IHSDT)**	0.216	0.020	15.381	0.690
		Present (TSDT)	0.217	0.020	15.352	0.715
		Wattanasakulpong and Ungbhakorn (2013)	0.203	0.020	15.530	0.723

4.3.1.4 Dimensionless axial displacement of CNT-Reinforced composite beam under various loads

The dimensionless axial displacement of a carbon nanotube reinforced composite beam under sinusoidal and uniformly distributed loading conditions provides valuable information about the structural response and behavior of the material. This analysis can help in understanding how the beam deforms and moves in response to varying loads, shedding light on the mechanical properties and performance of the composite material.

Figure 4.1 presents a graphical representation of the variation of non-dimensional axial displacement of simply supported carbon nanotube reinforced composite (CNTRC) beams when subjected to a sinusoidal and uniformly distributed load. The figure shows the variation of non-dimensional axial displacement of the CNTRC beam under (a) sinusoidal load and (b) UDL with inverse hyperbolic shear deformation theory and trigonometric shear deformation theory. The non-dimensional parameter for calculating the dimensionless axial displacements, denoted as $(\bar{u})$, is $\bar{u} = \frac{E_p u 100 h^3}{q_0 L^4}(0, \frac{L}{2})$. The non-dimensional axial displacement is plotted against the normalized thickness. This representation allows for a comparative analysis of the axial displacement behavior across the thickness of the beam under the applied load. These non-dimensional axial displacements are obtained for various CNTs distributions in a CNTRC beam for the length-to-thickness ratio of 10 and a volume fraction of 0.12. The figure likely shows the axial displacement for different beam configurations, such as UD (uniform distribution), FG-O Beam, and FG-X Beam. These configurations may refer to the distribution of carbon nanotubes within the composite beam, which can significantly influence the mechanical properties and displacement behaviour of the beam.

The figure illustrates the behavior of different beam configurations, specifically UD, FG-X, and FG-O Beams, which exhibit antisymmetrical distributions of carbon nanotubes (CNTs) along the mid-plane of the Carbon Nanotube Reinforced Composite (CNTRC) beam, as illustrated in **Figure 4.1**. At the mid-plane, the non-dimensional axial displacement is zero, indicating a symmetrical point where the displacements balance out in opposite directions. When examining the variation of non-dimensional axial displacement at the top edge of the beam, it is evident that the FG-O Beam distribution yields the highest values of this displacement. This suggests that the FG-O Beam configuration is particularly effective in maximizing axial displacement, likely due to its efficient load transfer or stress distribution properties. Additionally, it is observed that as the normalized thickness of the beam increases, the non-dimensional axial displacement also increases. This correlation implies that thicker beams undergo greater deformation under the same loading conditions, resulting in higher axial displacements. Overall, these observations highlight the significant impact of CNT distribution and beam thickness on the axial displacement behavior of CNTRC beams.

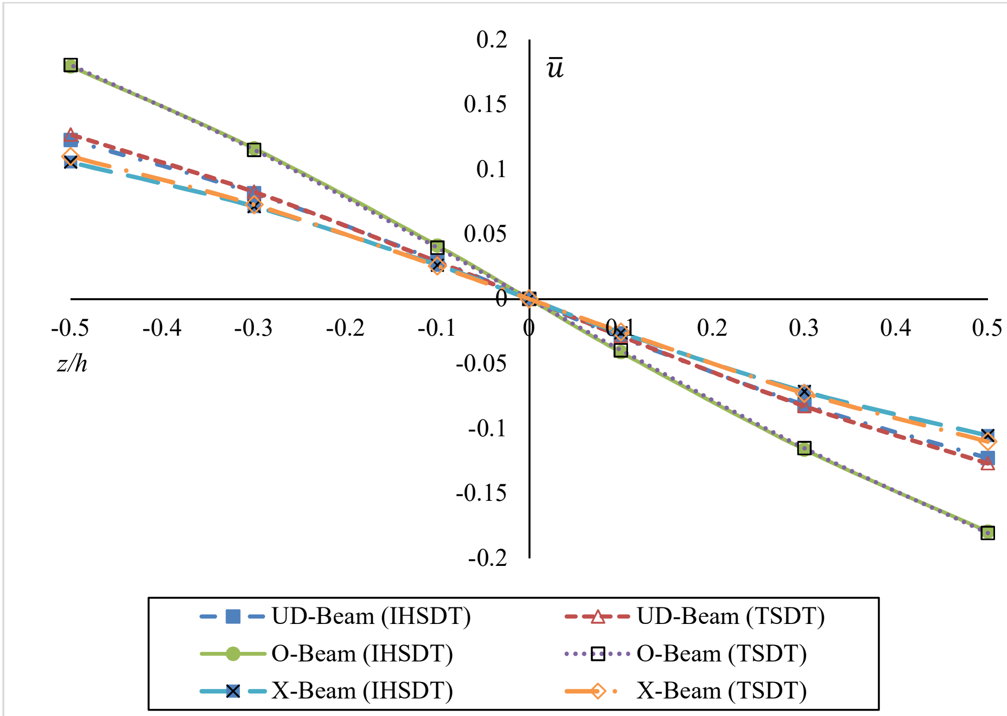

(a)

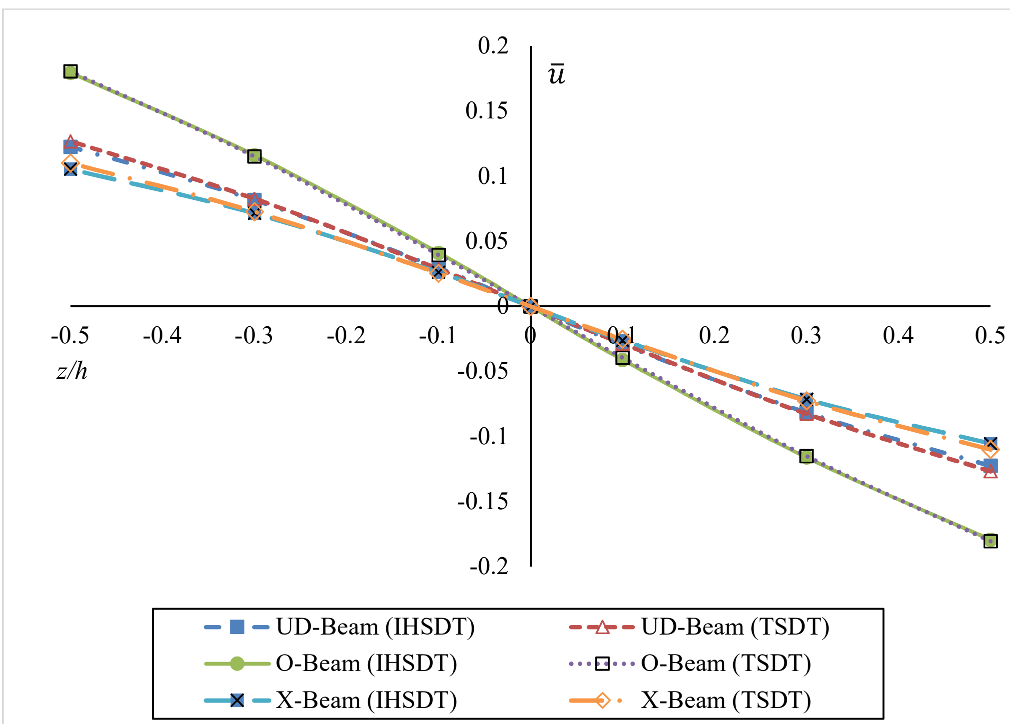

(b)

Figure 4.1. Variation of non-dimensional axial displacement of CNTRC beam under (a) sinusoidal load and (b) UDL with IHSDT and TSDT

4.3.1.5 Stress analysis of the composite beam reinforced with carbon nanotubes

This section provides a comprehensive discussion of the stress analysis of a carbon nanotube reinforced composite beam under various parametric conditions. The stress distribution of the beam is analyzed using an analytical approach. The effects of different span thickness ratios, volume fraction of carbon nanotubes (CNTs), and distribution of CNTs on the stress distribution are examined in detail. For the analysis, four different types of CNTs reinforcement distribution are considered. These include uniformly distributed (UD) CNTs, as well as three types of functionally graded (FG) CNTs distribution, namely FG-O, FG-X, and FG-V.

The objective is to determine the most optimal arrangement for the reinforcement distribution that will result in improved stress distribution responses for the functionally graded CNTs reinforced composite beam. The analytical analysis is based on the trigonometric shear deformation theory, which incorporates the secant and inverse sine functions. This approach allows for a more accurate representation of the behaviour of the beam under different loading conditions. By studying the stress distribution under various parametric conditions, valuable insights can be gained to enhance the design and performance of carbon nanotube reinforced composite beams.

4.3.1.5.1 Normal stress distribution in a composite beam reinforced with carbon nanotubes

The variation of dimensionless axial stress of Carbon Nanotube Reinforced Composite (CNTRC) beam under sinusoidal load and Uniform Distributed Load (UDL) conditions provides important insights into the structural response of the material. This analysis involves studying how the axial stress changes along the length of the beam when subjected to varying loading conditions. Understanding the variation of dimensionless axial stress helps in evaluating the behaviour of the material, determining critical locations for potential failure, and optimizing the design of CNTRC beams for enhanced performance and durability. **Figure 4.2** illustrates the variation of dimensionless axial stress in a Carbon Nanotube Reinforced Composite (CNTRC) beam under sinusoidal loading and UDL conditions, considering two different shear deformation theories. The figure shows the variation of non-dimensional axial stress of the CNTRC beam under (a) sinusoidal load and (b) UDL with inverse hyperbolic shear deformation theory and trigonometric shear deformation theory. The analysis is conducted with a span-to-thickness ratio (*L/h*) of 10 and a volume fraction of carbon nanotubes (V_{cnt}^*) of 0.12. The non-dimensional parameter for calculating the dimensionless axial stress of a simply supported CNTRC beam is given by $\bar{\sigma}_{xx} = \frac{h}{q_0 L}\, \sigma_{xx}(\frac{L}{2}, \frac{h}{2})$.

The figure shows that the UD (Uniform Distribution), FG-X, and FG-O Beams exhibit symmetrical distributions of CNTs both before and after the mid-plane of the CNTRC beam. This symmetry implies that the material properties and the reinforcement provided by the CNTs are mirrored along the mid-plane, leading to a balanced structural behavior under loading conditions. One critical observation from the figure is that the dimensionless normal stresses at the mid-plane of the CNTRC beam are zero. This indicates a point of equilibrium where the compressive and tensile stresses cancel each other out. The zero-stress value at the mid-plane is a characteristic of symmetric loading and material distribution, ensuring that there is no net normal stress at this central point. The fluctuation of dimensionless normal stresses before and after the mid-plane is equal in magnitude but different in nature. This means that the normal stresses exhibit the same absolute values but opposite signs on either side of the mid-plane. For instance, if the stress is tensile above the mid-plane, it is compressive below the mid-plane, and vice versa. When examining the variation of dimensionless normal stresses at the upper edge of the beam, it is observed that the FG-O Beam distribution results in the lowest values of normal stress.

This finding is significant as it suggests that the FG-O Beam configuration is particularly effective in minimizing normal stresses at the extreme fiber of the beam, where stresses typically reach their maximum values. The reduced normal stress in the FG-O Beam configuration could be attributed to the specific arrangement and orientation of CNTs, which enhance the load-carrying capacity and distribute the stresses more efficiently across the cross-section of the beam.

4.3.2 Buckling analysis of carbon nanotube reinforced composite beam

Buckling analysis is a critical aspect of structural engineering, particularly for slender members like beams, where failure can occur due to instability under compressive loads. For Carbon Nanotube Reinforced Composite (CNTRC) beams, the presence of carbon nanotubes (CNTs) significantly influences their buckling behavior, offering enhanced mechanical properties such as increased stiffness and strength. The critical buckling load is the maximum axial load a beam can withstand before buckling. CNTRC beams typically exhibit higher critical buckling loads compared to conventional composite beams due to the reinforcing effect of CNTs.

4.3.2.1 Buckling analysis of the CNT-Reinforced composite beam under uniaxial compression

The critical buckling load is a fundamental parameter in structural engineering, as it indicates the maximum load a beam can withstand before it becomes unstable and potentially fails due to buckling. The discussion focuses on the critical buckling load of simply supported carbon nanotube reinforced composite (CNTRC) beams subjected to uniaxial compressive load with a length-to-thickness ratio (*L/h*) of 15 and varying the volume fraction of carbon nanotubes (CNTs) as presented in **Table 4.7.**

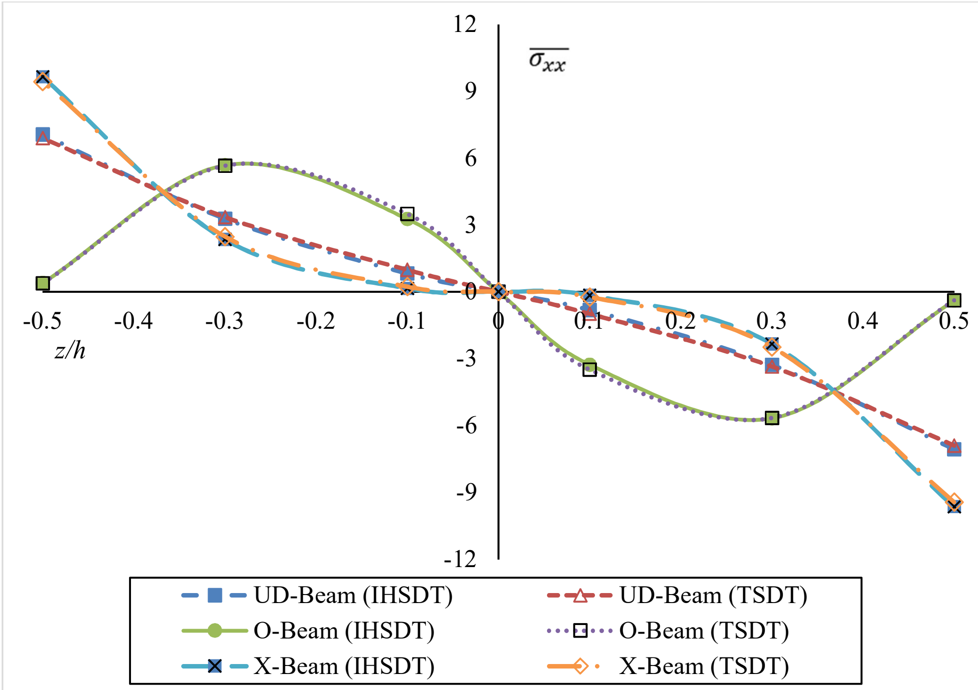

(a)

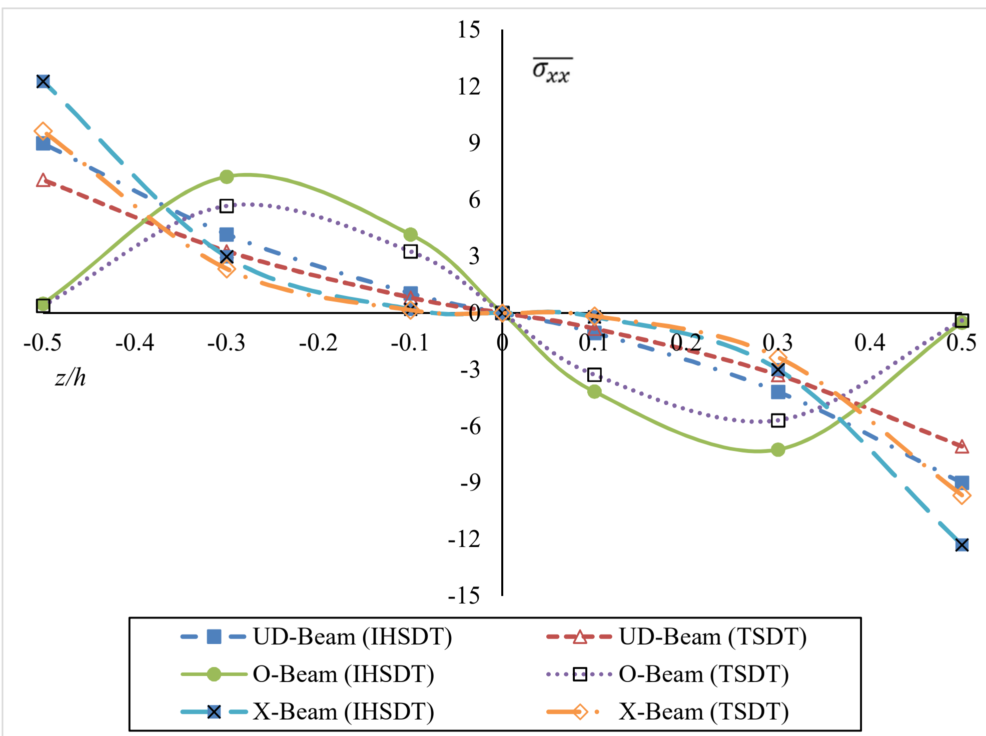

(b)

Figure 4.2. Variation of dimensionless axial stress of CNTRC beam under (a) sinusoidal load and (b) UDL with IHSDT and TSDT (L/h = 10; V_{cnt}^{*} = 0.12

The table also provides a comparative analysis of the critical buckling load for carbon nanotube reinforced composite (CNTRC) beams with different fiber distributions. The analytical solution approach is used with the help of the Naviers solution technique. The non-dimensional parameter for calculating the critical buckling load of CNTRC beam is given by $\bar{N}_{x0} = \frac{N_{cr}}{A_{110}}$.

The table is structured to compare the critical buckling load for four types of CNTRC beams: UD (uniform distribution), FG-O Beam, FG-X Beam, and FG-V Beam. These distributions likely refer to the arrangement of carbon nanotubes within the composite material, which can significantly influence the mechanical properties and load-carrying capacity of the beam. The critical buckling load is presented for two different shear deformation theories used in the analysis and are compared with the results of Yas and Samadi (2012) based on Timoshenko beam theory (TBT), Karamanli and Vo (2011) based on shear and normal deformation theory (SNDT) and Kumar and Srinivas (2017) based on First order Shear Deformation Theory.

It is observed from the table that the presented results show good agreement with the compared results available in the existing literature. The table also compares the results obtained using different theoretical models to evaluate the buckling load. This comparison is essential to validate the accuracy and reliability of the analytical approaches used. The critical buckling load increases with the volume fraction of CNTs (V_{cnt}^{*}). This trend underscores the role of CNTs in reinforcing the composite material, providing improved stiffness and strength, which are crucial for resisting buckling.

The table indicates that an increase in the volume fraction of CNTs in a CNTRC beam results in a corresponding rise in the non-dimensional critical buckling load under uniaxial compressive load. Similarly, for an unsymmetrical FG-V distribution, it is observed that the non-dimensional critical buckling load of a CNTRC beam under uniaxial compressive load increases as the volume fraction of CNTs in the beam increases. It is easy to detect that the FG-O reinforcing distribution pattern of CNTs throughout the thickness of the CNTRC beam yields the lowest resistance non-dimensional critical buckling load under uniaxial compressive load. The maximum resistance to the non-dimensional critical buckling load under uniaxial compressive stress is produced by the FG-X reinforcement distribution pattern of CNTs throughout the thickness of the CNTRC beam.

Table 4.7 CNTRC beams critical buckling load (*L/h* =15)

V_{cnt}^{*}	Source	UD	FG-V Beam	FG-O Beam	FG-X Beam
	Present (IHSDT)	0.093	0.070	0.054	0.124
0.12	**Present (TSDT)**	0.092	0.069	0.053	0.122
	TBT*	0.099	0.093	0.059	0.129
	SNDT**	0.098	-	0.059	0.129
	FSDT#	0.108	0.102	0.064	0.141
	Present (IHSDT)	0.142	0.105	0.081	0.190
0.17	**Present (TSDT)**	0.141	0.104	0.081	0.188
	TBT*	0.151	0.141	0.088	0.200
	SNDT**	0.150	-	0.086	0.198
	FSDT#	0.166	0.155	0.096	0.220
	Present (IHSDT)	0.211	0.158	0.125	0.268
0.28	**Present (TSDT)**	0.209	0.157	0.125	0.266
	TBT*	0.221	0.209	0.134	0.290
	SNDT**	0.220	-	0.133	0.276
	FSDT#	0.242	0.230	0.147	0.317

*Yas and Samadi (2012), **Karamanli and Vo (2021), #Kumar and Srinivas (2017)

The critical buckling load results for a Carbon Nanotube Reinforced Composite (CNTRC) beam with a volume fraction of 0.12 and a span-to-thickness ratio of 15 have been compared with the results from various deformation theories provided by Wattanasakulpong and Ungbhakorn (2013), and Yas and Samadi (2012), as shown in **Table 4.8**. The present study's results align well with these previously reported results, indicating the validity and accuracy of the current analysis. The FG-V Beam, due to its inherent asymmetry, displays unique stretching-bending coupling properties. This coupling effect means that when the V-Beam is subjected to compressive loads, it experiences not just direct axial compression but also deflections and bending moments. This phenomenon occurs because the asymmetrical distribution of CNTs leads to differential stiffness across the cross-section of the beam, causing the beam to bend and stretch simultaneously under compression. As a result, the FG-V Beam does not undergo the traditional bifurcation-type buckling, where the beam would typically exhibit a sudden change in deformation pattern at the critical load. Instead, the FG-V Beam response to compressive loading is more complex and involves a gradual increase in deflections and bending moments.

In the present analysis, the FG-X Beam is found to be the strongest among the compared beam types (FG-X Beam, UD-Beam, and FG-O Beam). The FG-X Beam can carry the maximum buckling load, indicating its superior stability and resistance to buckling under compressive loads. This superior performance is likely due to the optimal distribution and orientation of CNTs in the FG-X Beam, which enhances its stiffness and load-bearing capacity.

Table 4.8 Non-dimensional buckling load for different distributions of CNTRC beam

Source	UD	FG-O Beam	FG-X Beam
Present (IHSDT)	0.0934	0.0536	0.1242
Present (TSDT)	0.0927	0.0538	0.1225
TSDT*	0.0984	0.0576	0.1289
ESDT*	0.0987	0.0574	0.1295
HSDT*	0.0984	0.0576	0.1288
TrSDT*	0.0985	0.0575	0.1291
FSDT*	0.1032	0.0604	0.1367
TBT**	0.0986	0.0588	0.1288

*Wattanasakulpong and Ungbhakorn (2013), **Yas and Samadi (2012)

The analysis of functionally graded Carbon Nanotube Reinforced Composite (FG-CNTRC) beams reveals important insights into their critical buckling behavior under various volume fractions of CNTs and different span-to-thickness (*L/h*) ratios. The non-dimensional parameter for calculating the critical buckling load of a simply supported CNTRC beam is given by $\bar{N}_{x0} = \frac{N_{cr}}{A_{110}}$.

The results, illustrated in **Figure 4.3**, highlight how the distribution of CNTs across the beam cross-section affects its stability and load-bearing capacity. **Figure 4.3** depicts various configurations of CNT reinforcement across the beam cross-section for different FG-CNTRC beams. The analysis compares different distribution patterns: UD (Uniform Distribution), FG-O, FG-X and FG-V. One of the key observations is that the FG-X distribution pattern achieves the highest critical buckling load among all the distribution types. This indicates that the FG-X configuration is the most effective in enhancing the stability of the beam under compressive loads. Additionally, the critical buckling load increases with the volume percentage of CNTs. This trend highlights the reinforcing effect of CNTs, where higher concentrations of CNTs result in greater stiffness and, consequently, higher resistance to buckling. The critical buckling load for different CNT distribution patterns (UD, FG-O, FG-X, FG-V) is presented in relation to the *L/h* ratio. The *L/h* ratio is a crucial factor influencing the buckling behavior of beams. As the *L/h* ratio increases, the critical buckling load decreases. This is because a higher *L/h* ratio indicates a more slender beam, which is more prone to buckling under compressive loads. Slender beams have lower critical buckling loads due to their reduced stiffness and higher susceptibility to instability. The graph indicates a notable variation in the critical buckling load when the *L/h* ratio ranges between 15 and 30.

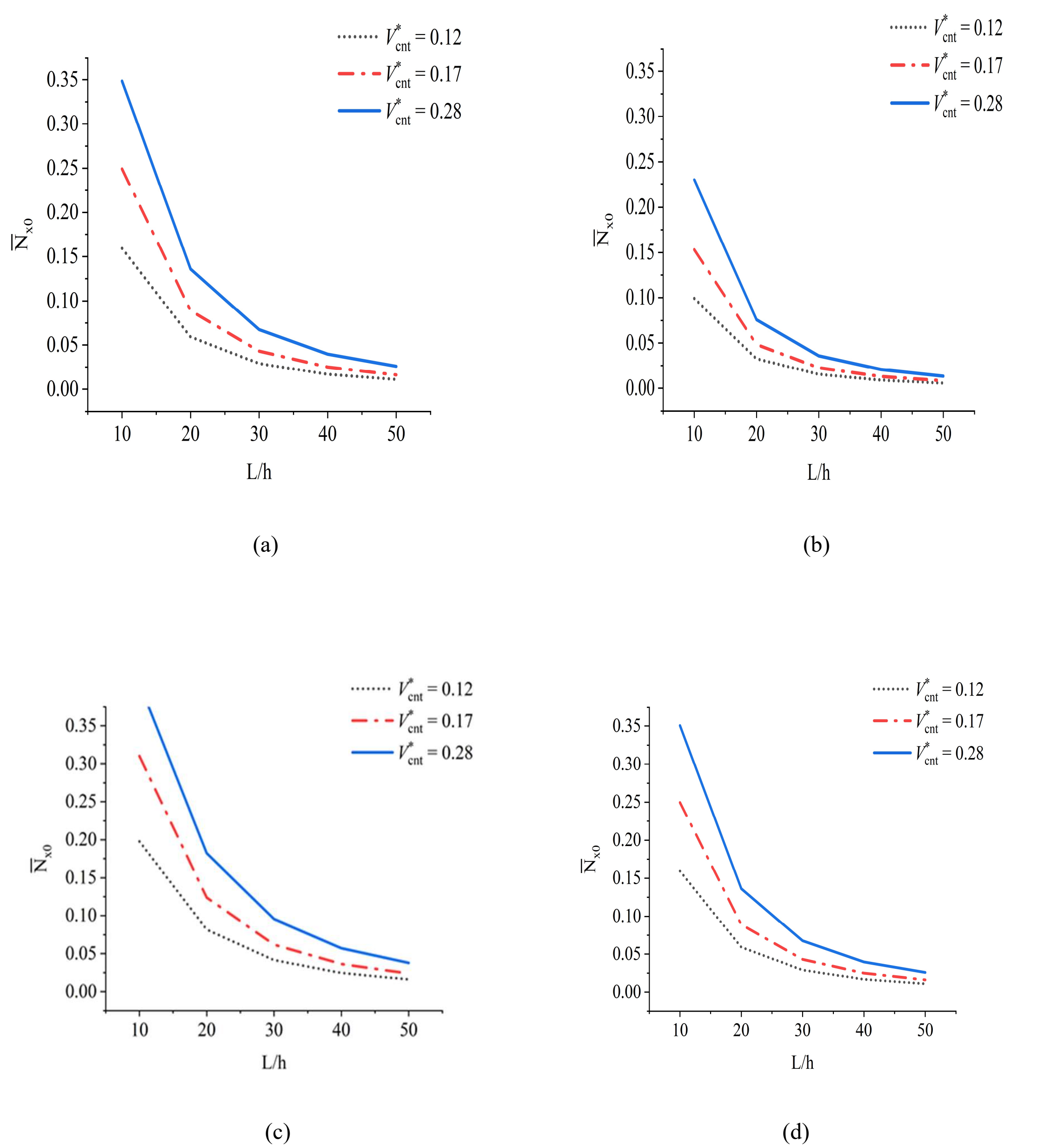

Figure 4.3. Critical buckling load of (a) UD-Beam, (b) FG-O Beam, (c) FG-X Beam, and (d) FG-V Beam

4.3.3 Free Vibration analysis of carbon nanotube reinforced composite beam

This section investigates the dynamic behavior of a simply supported carbon nanotube reinforced composite (CNTRC) beam by analyzing the effects of various parameters such as CNT volume fractions, length-to-thickness ratios, and CNT distribution patterns on the non-dimensional natural frequency. The governing equations for this dynamic analysis are derived using trigonometric shear deformation theory based on the secant and inverse sine functions. Utilizing Navier's solution technique, an analytical approach is applied to determine the dynamic behavior of the CNTRC beam under these conditions. A span-to-thickness ratio of 15 is employed to compute the non-dimensional natural frequency, considering different volume fractions of CNTs, specifically. V_{cnt}^{*} = 0.12, 0.17, and 0.28, along with various distribution patterns of CNTs across the beam. The non-dimensional parameter for calculating the dimensionless natural frequency of a simply supported CNTRC beam is given by $\overline{\omega} = \omega L \sqrt{\frac{I_{00}}{A_{110}}}$.

By using the trigonometric shear deformation theory based on the secant and inverse sine functions the obtained natural frequency results are compared with those from previous studies, including Timoshenko Beam Theory (TBT), by Yas and Samadi (2012), shear and normal deformation theory (SNDT) by Karamanli and Vo (2021), and First-order Shear Deformation Theory (FSDT) by Kumar and Srinivas (2017) as shown in **Table 4.9** this comparison indicates a strong agreement between the presented results and the existing data.

For a specific length-to-thickness ratio and different CNT volume fractions in the CNTRC beam, the non-dimensional natural frequency is found to be lowest for the FG-O Beam configuration and highest for the FG-X Beam configuration. Additionally, for a particular volume fraction of CNTs and a specific length-to-thickness ratio, the highest non-dimensional natural frequency is observed in the FG-X Beam, followed sequentially by the UD (uniformly distributed) Beam, the FG-V Beam, and the FG-O Beam. This highlights the significant influence of CNT distribution patterns on the dynamic properties of the CNTRC beam, with the FG-X Beam configuration providing the most effective reinforcement in terms of increasing the natural frequency.

Table 4.9 Non-dimensional natural frequency of CNTRC beam (*L/h* =15)

V^*_{cnt}	Source	UD	FG-V Beam	FG-O Beam	FG-X Beam
	Present (IHSDT)	0.952	0.822	0.721	1.097
0.12	**Present (TSDT)**	0.948	0.819	0.722	1.089
	TBT*	0.975	0.945	0.753	1.115
	SNDT**	0.975	0.944	0.745	1.115
	FSDT#	1.024	0.994	0.791	1.171
	Present (IHSDT)	1.170	1.003	0.880	1.353
0.17	**Present (TSDT)**	1.166	1.001	0.882	1.346
	TBT*	1.200	1.161	0.916	1.383
	SNDT**	1.198	1.158	0.909	1.376
	FSDT#	1.260	1.220	0.962	1.451
	Present (IHSDT)	1.410	1.220	1.085	1.590
0.28	**Present (TSDT)**	1.404	1.217	1.084	1.585
	TBT*	1.440	1.402	1.120	1.649
	SNDT**	1.436	1.393	1.115	1.611
	FSDT#	1.509	1.471	1.176	1.726

*Yas and Samadi (2012), **Karamanli and Vo (2021), #Kumar and Srinivas (2017)

The dynamic behavior of a simply supported carbon nanotube reinforced composite (CNTRC) beam is analyzed by considering a specific volume fraction of 0.12 and a span-to-thickness ratio of 15. The non-dimensional natural frequency results for this beam are compared to those obtained using various deformation theories, including the Timoshenko Beam Theory (TBT) as provided by Wattanasakulpong and Ungbhakorn (2013), and Yas and Samadi (2012). These comparisons are presented in **Table 4.10.**

The table shows that the results derived from different deformation theories are in strong agreement with the results obtained using trigonometric shear deformation theory based on the secant and inverse sine functions. It is observed that, for the given volume fraction of CNTs and length-to-thickness ratio, the non-dimensional natural frequency is the lowest for the FG-O Beam distribution pattern and the highest for the FG-X Beam distribution pattern. In dynamic analysis, the FG-X Beam configuration is identified as the strongest, exhibiting the maximum non-dimensional natural frequency. This is followed by the UD (uniformly distributed) Beam, the FG-V Beam, and lastly, the FG-O Beam. This indicates that the distribution pattern of CNTs significantly influences the dynamic properties of the CNTRC beam, with the FG-X Beam providing the most effective reinforcement in terms of natural frequency.

Table 4.10 Comparative of non-dimensional natural frequencies for various distributions for CNTRC beam (L/h = 15; V_{cnt}^{*} = 0.12)

Source	UD	FG-O Beam	FG-X Beam	FG-V Beam
Present (IHSDT)	0.9516	0.7210	1.0972	0.8221
Present (TSDT)	0.9480	0.7226	1.0896	0.8199
TSDT*	0.9745	0.7453	1.1152	0.8441
ESDT*	0.9756	0.7440	1.1180	0.8448
HSDT*	0.9745	0.7454	1.1151	0.8441
TrSDT*	0.9749	0.7446	1.1163	0.8443
FSDT*	0.9976	0.7628	1.1485	0.8592
TBT**	0.9753	0.7527	1.1150	0.9453

*Wattanasakulpong and Ungbhakorn (2013), **Yas and Samadi (2012)

Figure 4.4 illustrates the fundamental frequency of carbon nanotube reinforced composite (CNTRC) beams under varying conditions: different volume fractions of CNTs, length-to-thickness ratios, and configurations of CNT reinforcement across the cross-section of the beam. This analysis is crucial for understanding how these factors influence the dynamic behavior of CNTRC beams, which is vital for their application in engineering structures where vibrational performance is a key concern.

The non-dimensional natural frequency of the CNTRC beam exhibits a clear dependency on the length-to-thickness ratio (L/h). As the ratio increases, the fundamental frequency decreases. This trend indicates that beams with higher length-to-thickness ratios (longer and thinner beams) are more prone to lower vibrational frequencies, which can be attributed to reduced stiffness and increased flexibility. When examining the effect of CNT volume fraction (V_{cnt}^{*}), it is evident that the fundamental frequency of the CNTRC beam increases with higher CNT content. This increase in frequency can be attributed to the enhanced stiffness and material properties provided by the CNTs, which reinforce the beam structure and improve its dynamic response. The behavior of the CNTRC beams under vibrational analysis mirrors trends observed in buckling analysis. Specifically, increasing the span-to-thickness ratio (*L/h*) reduces both the natural frequency and buckling load. Similarly, increasing the CNT volume fraction enhances both the natural frequency and buckling resistance. The non-dimensional parameter for calculating the dimensionless natural frequency of a simply supported CNTRC beam is given by $\overline{\omega} = \omega L\sqrt{\frac{I_{00}}{A_{110}}}$.

The results depicted in **Figure 4.4** underline the significant impact of CNT distribution patterns on the dynamic properties of CNTRC beams. The FG-X Beam configuration demonstrates the highest efficiency in enhancing natural frequencies, making it the optimal choice for maximizing dynamic performance. In contrast, the FG-O Beam configuration, while potentially beneficial for other mechanical properties or design considerations, shows the lowest natural frequencies. The UD Beam offers a balanced performance, serving as a reliable standard, while the FG-V Beam provides an intermediate option.

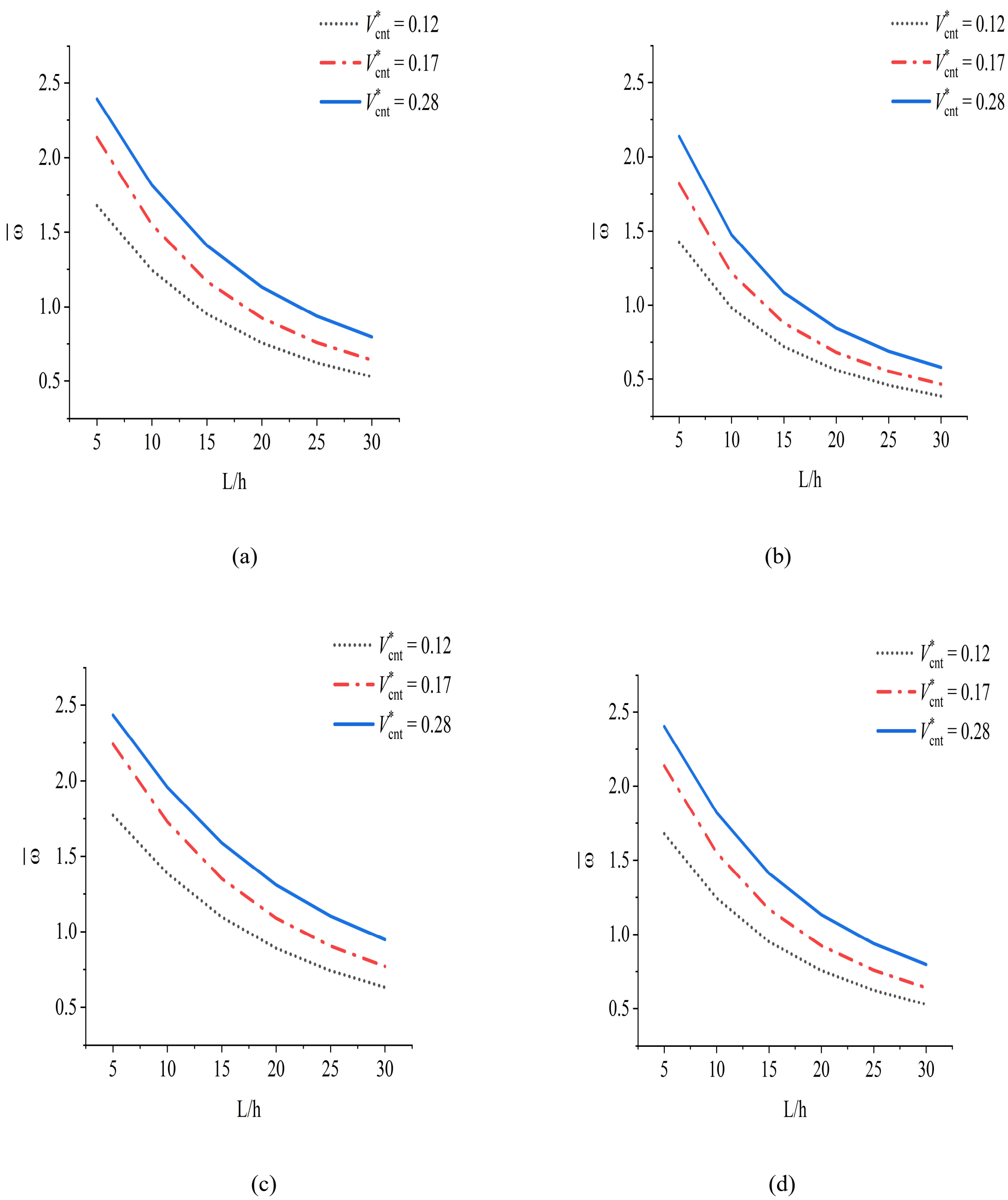

Figure 4.4. Fundamental frequency of (a) UD-Beam, (b) FG-O Beam, (c) FG-X Beam, and (d) FG-V Beam

4.4 Structural analysis of functionally graded carbon nanotube reinforced composite beams resting on the Pasternak elastic foundation

This section provides an in-depth analysis of the bending, buckling, and free vibration behaviors of functionally graded carbon nanotube reinforced composite (FG-CNTRC) beams. These beams are supported by a Pasternak elastic foundation, which includes both a shear layer and Winkler springs. The study utilizes a non-polynomial shear deformation theory, specifically employing secant and inverse hyperbolic sine functions to model the deformation. This theory ensures that the traction-free boundary conditions at the top and bottom surfaces of the beam are accurately fulfilled. To derive the governing differential equations for the FG-CNTRC beams on the Pasternak elastic foundation, Hamilton's principle is employed. This principle is fundamental in mechanics and ensures that the derived equations reflect the physical behavior of the system. The study applies Navier's technique to solve the governing equations, particularly under simply supported boundary conditions. These methods are well-established for their accuracy and efficiency in solving complex differential equations in structural mechanics and offering a novel approach to understanding the structural behavior of CNTRC beams under various conditions. Different volume fractions of carbon nanotubes (CNTs) are considered to study their effect on the mechanical properties of the beams. Higher CNT content generally enhances the stiffness and strength of the composite material.

The distribution pattern of CNTs within the matrix is another critical factor. The study explores various reinforcement and resin combinations to optimize the structural performance of the beams. The effects of varying spring constants in the Pasternak foundation model are examined to determine their impact on the structural responses of the beam. Numerical examples are provided to analyze the bending behavior of CNTRC beams under transverse loading (SSL) and uniformly distributed load (UDL). The results demonstrate how span-to-thickness ratios and CNT volume fractions influence the transverse deflections and stresses. The buckling behavior under uniaxial in-plane load is examined. The study reveals how different CNT configurations and span-to-thickness ratios impact the critical buckling loads. The natural frequencies of the beams are computed to understand their free vibration response. The analysis highlights the effect of CNT distribution and volume fractions on the vibrational characteristics. The mechanical characteristics of the CNTRC beam are changed by the distribution of CNTs in the matrix. The research analyses different reinforcement and resin combinations to improve the structural performance of a composite beam.

The selection of Poly methyl methacrylate (PMMA) as the matrix material and armchair (10,10) as the reinforcement material is based on the fact that PMMA has a strong bonding capability and armchair (10,10) has a high impact resistance. The bond strength between single-walled carbon nanotubes (SWCNTs) and PMMA is determined using molecular dynamics simulations. This analysis helps in understanding the interaction between the reinforcement and matrix materials. The results obtained from the simulations are compared with published data derived from different theories. This comparison validates the accuracy of the proposed model and the effectiveness of the material combinations used.

4.4.1 Static analysis of FG-CNT reinforced beams on the Pasternak elastic foundation

The study focuses on the bending responses of functionally graded carbon nanotube reinforced composite (CNTRC) beams resting on a Pasternak elastic foundation. This analysis is comprehensive, covering various aspects such as transverse deflection, normal stresses, and shear stresses. The effects of several key parameters, including the volume fraction of CNTs, distribution patterns of CNTs, length-to-thickness ratio, and spring constant factors, are examined in detail.

4.4.1.1 Dimensionless transverse deflection and stress of FG-CNT reinforced beams on the Pasternak foundation under sinusoidal load

In this study, the static analysis of a sinusoidally loaded, uniformly distributed (UD), simply supported functionally graded carbon nanotube reinforced composite (FG-CNTRC) beam with the Pasternak elastic foundation is conducted. The foundation model incorporates both Winkler springs and a shear layer to account for elastic support characteristics. The analysis calculates the dimensionless transverse displacement, axial displacement, and normal stresses for various CNT distributions, length-to-thickness ratios, and CNT volume fractions within FG-CNTRC beams. In addition to the FG-O, FG-V, and FG-X distributions, the UD distribution is employed for comparative analysis. The non-dimensional parameter for calculating the dimensionless displacements and stress of CNTRC beam resting on an elastic foundation is given by $\bar{w} = \frac{E_p w 100 h^3}{q_0 L^4}\left(\frac{L}{2}\right)$, $\bar{u} = \frac{E_p u 100 h^3}{q_0 L^4}(0, \frac{L}{2})$, $\bar{\sigma}_{xx} = \frac{h}{q_0 L}\sigma_{xx}(\frac{L}{2}, \frac{h}{2})$, $\bar{\sigma}_{xz} = \frac{h}{q_0 L}\sigma_{xz}(0,0)$. The study considers varying span-to-thickness ratios (*L/h*) and three different CNT volume fractions (V_{cnt}^*) of the beams with Winkler springs and a shear layer constant values of β_w = 0.1 and β_s = 0.02 respectively.

The non-polynomial shear deformation theory, specifically employing secant and inverse hyperbolic sine functions is utilized to represent the dimensionless deflection and stresses of the UD beam under sinusoidal loading conditions. The results are compared with those obtained by Wattanasakulpong and Ungbhakorn (2013), who used the Third Order Shear Deformation Theory (TSDT). **Table 4.11** displays the non-dimensional central deformation, dimensionless axial deflection, non-dimensional normal stress, and dimensionless transverse shear stresses at the critical point. The analysis shows that the dimensionless transverse deflection and axial displacement decrease with an increasing span-to-thickness ratio. This indicates that beams with higher *L/h* ratios exhibit less transverse and axial deflection under sinusoidal loading conditions. Similarly, an increase in the CNT volume fraction results in decreased dimensionless transverse deflection and axial displacement. This reflects enhanced stiffness and reduced deformation due to the higher CNT content, which improves the load-bearing capacity of the beam. On the other hand, the dimensionless axial stresses increase with both the CNT volume fraction and the *L/h* ratio. This suggests that beams with higher CNT content and higher *L/h* ratios experience greater internal forces, leading to increased axial stress. For the lowest span-to-thickness ratio and the lowest CNT volume fraction, the table shows the maximum non-dimensional transverse displacement and axial displacement. This confirms that lower CNT content and lower *L/h* ratios correspond to higher deformation levels, indicating a less stiff structure.

Table 4.11 Dimensionless stresses and displacements of UD-Beams under sinusoidal loading condition. ($\beta_w = 0.1$, β_s= 0.02)

V^*_{CNT}	*L/h*	Theory	$\bar{w}$	$\bar{u}$	$\bar{\sigma}_{xx}$	$\bar{\sigma}_{xz}$
0.12	10	**Present (IHSDT)**	0.486	0.103	5.937	-
		Present (TSDT)	0.493	0.106	5.788	0.397
		Wattanasakulpong and Ungbhakorn (2013)	0.475	0.104	5.890	0.399
	15	**Present (IHSDT)**	0.331	0.041	7.394	-
		Present (TSDT)	0.334	0.043	7.296	0.359
		Wattanasakulpong and Ungbhakorn (2013)	0.319	0.041	7.439	0.364
	20	**Present (IHSDT)**	0.258	0.022	8.388	-
		Present (TSDT)	0.259	0.023	8.320	0.315
		Wattanasakulpong and Ungbhakorn (2013)	0.247	0.022	8.535	0.322
0.17	10	**Present (IHSDT)**	0.330	0.068	6.176	-
		Present (TSDT)	0.334	0.070	6.044	0.422
		Wattanasakulpong and Ungbhakorn (2013)	0.321	0.068	6.126	0.424
	15	**Present (IHSDT)**	0.237	0.029	7.994	-

		Present (TSDT)	0.239	0.030	7.906	0.392
		Wattanasakulpong and Ungbhakorn (2013)	0.227	0.029	8.021	0.396
	20	**Present (IHSDT)**	0.193	0.016	9.404	-
		Present (TSDT)	0.194	0.017	9.341	0.356
		Wattanasakulpong and Ungbhakorn (2013)	0.184	0.016	9.520	0.362
0.28	10	**Present (IHSDT)**	0.243	0.052	6.668	-
		Present (TSDT)	0.248	0.055	6.485	0.434
		Wattanasakulpong and Ungbhakorn (2013)	0.239	0.054	6.573	0.435
	15	**Present (IHSDT)**	0.170	0.020	8.667	-
		Present (TSDT)	0.172	0.022	8.542	0.415
		Wattanasakulpong and Ungbhakorn (2013)	0.164	0.022	8.639	0.418
	20	**Present (IHSDT)**	0.138	0.012	10.438	-
		Present (TSDT)	0.139	0.013	10.346	0.389
		Wattanasakulpong and Ungbhakorn (2013)	0.133	0.012	10.485	0.393

4.4.1.2 Dimensionless transverse deflection and stress of FG-CNT reinforced beams on the Pasternak foundation under uniformly distributed load

The static analysis of a uniformly distributed load (UDL) on a simply supported, uniformly distributed (UD), functionally graded carbon nanotube reinforced composite (FG-CNTRC) beam with the Pasternak elastic foundation is carried out in this work. To account for the elastic support properties, the foundation model includes a shear layer in addition to Winkler springs. The dimensionless transverse displacement, axial displacement, and normal stresses within FG-CNTRC beams are calculated for different CNT distributions, length-to-thickness ratios, and CNT volume fractions. For comparative study, the UD distribution is used in addition to the FG-O, FG-V, and FG-X distributions. The non-dimensional parameter for calculating the dimensionless displacements and stress of the CNTRC beam resting on an elastic foundation is given by $\bar{w} = \frac{E_p w 100 h^3}{q_0 L^4}\left(\frac{L}{2}\right)$, $\bar{u} = \frac{E_p u 100 h^3}{q_0 L^4}\left(0, \frac{L}{2}\right)$,$\bar{\sigma}_{xx} = \frac{h}{q_0 L}\sigma_{xx}(\frac{L}{2}, \frac{h}{2})$, $\bar{\sigma}_{xz} = \frac{h}{q_0 L}\sigma_{xz}(0,0)$. The research takes into account three distinct CNT volume fractions (V_{cnt}^*) and varying span-to-thickness ratios (*L/h*) for the beams equipped with Winkler springs, as well as shear layer constant values of β_w = 0.1 and β_s = 0.02, respectively.

The dimensionless deflection and stresses of the UD beam under the uniformly distributed loading condition are represented by the non-polynomial shear deformation theory, which specifically uses secant and inverse hyperbolic sine functions. Wattanasakulpong and Ungbhakorn (2013) employed the Third Order Shear Deformation Theory (TSDT) to obtain their results, which are compared to ours. **Table 4.12** shows the dimensionless transverse shear stresses, non-dimensional normal stress, non-dimensional axial deflection, and non-dimensional central deformation at the critical point. According to the analysis, as the span-to-thickness ratio increases, the dimensionless transverse deflection and axial displacement decrease. This suggests that under uniformly distributed loading conditions, longer and thinner beams with larger *L/h* ratios exhibit less axial and transverse displacement. Similarly, both axial displacement and dimensionless transverse deflection decrease with an increase in the CNT volume percentage. This indicates increased stiffness and decreased deformation as a result of the higher CNT content, enhancing the load-bearing capacity of the beam. Conversely, the dimensionless axial stresses rise with an increase in both the *L/h* ratio and the CNT volume percentage. This indicates that higher *L/h* ratios and CNT content in beams lead to greater internal forces and increased axial stress. The table shows the maximum non-dimensional transverse displacement and axial displacement for the lowest span-to-thickness ratio and the lowest CNT volume fraction. This illustrates that a less rigid structure is indicated by higher deformation levels corresponding to lower *L/h* ratios and lower CNT content.

Table 4.12 Dimensionless stresses and displacements of UD-Beams under UDL conditions ($\beta_w = 0.1$, β_s= 0.02)

V^*_{CNT}	*L/h*	Theory	$\bar{w}$	$\bar{u}$	$\bar{\sigma}_{xx}$	$\bar{\sigma}_{xz}$
0.12	10	**Present (IHSDT)**	0.619	0.131	7.550	0.571
		Present (TSDT)	0.627	0.135	7.369	0.564
		Wattanasakulpong and Ungbhakorn (2013)	0.594	0.148	7.053	0.602
	15	**Present (IHSDT)**	0.422	0.053	9.414	0.539
		Present (TSDT)	0.424	0.054	9.289	0.523
		Wattanasakulpong and Ungbhakorn (2013)	0.400	0.058	9.556	0.568
	20	**Present (IHSDT)**	0.328	0.029	10.680	0.519
		Present (TSDT)	0.329	0.029	10.593	0.513
		Wattanasakulpong and Ungbhakorn (2013)	0.311	0.031	10.316	0.520
0.17	10	**Present (IHSDT)**	0.420	0.089	7.764	0.608
		Present (TSDT)	0.425	0.089	7.651	0.599
		Wattanasakulpong and Ungbhakorn (2013)	0.403	0.097	7.374	0.638
	15	**Present (IHSDT)**	0.302	0.039	10.100	0.593
		Present (TSDT)	0.304	0.038	10.066	0.589
		Wattanasakulpong and Ungbhakorn (2013)	0.286	0.040	9.736	0.614
	20	**Present (IHSDT)**	0.246	0.021	11.974	0.556
		Present (TSDT)	0.246	0.021	11.893	0.539
		Wattanasakulpong and Ungbhakorn (2013)	0.232	0.022	11.568	0.575
0.28	10	**Present (IHSDT)**	0.310	0.067	8.491	0.623
		Present (TSDT)	0.315	0.069	8.257	0.615

	Wattanasakulpong and Ungbhakorn (2013)	0.299	0.076	7.869	0.647
15	**Present (IHSDT)**	0.216	0.028	11.035	0.601
	Present (TSDT)	0.218	0.028	10.875	0.597
	Wattanasakulpong and Ungbhakorn (2013)	0.206	0.030	10.469	0.638
20	**Present (IHSDT)**	0.176	0.015	13.291	0.564
	Present (TSDT)	0.177	0.016	13.171	0.539
	Wattanasakulpong and Ungbhakorn (2013)	0.167	0.017	12.751	0.613

4.4.1.3 Dimensionless axial displacement of CNT-Reinforced beam on the Pasternak foundation under various loads

A carbon nanotube reinforced composite beam under sinusoidal and uniformly distributed loading conditions, resting on the Pasternak elastic foundation, can reveal important details about the behavior of the material and structural response through its dimensionless axial displacement. This analysis can illuminate the mechanical characteristics and performance of the composite material, aiding in the understanding of how the beam deforms and responds to varying loads. **Figure 4.5** illustrates the dimensionless axial displacements for a simply supported FG-CNTRC beam with an elastic foundation under sinusoidal and uniformly distributed loading conditions. The figure shows the variation of non-dimensional axial displacement of the CNTRC beam with an elastic foundation under (a) sinusoidal load and (b) UDL with inverse hyperbolic shear deformation theory and trigonometric shear deformation theory.

This figure provides insights into how different carbon nanotube (CNT) distributions within the beam affect its deformation behavior. The dimensionless axial displacements are obtained for normalized thicknesses, allowing for comparative analysis across different beam configurations. In this study, the span-to-thickness ratio is held constant at 10, while the CNT volume fraction is set at 0.12. The non-dimensional parameter for calculating the dimensionless axial displacements of the CNTRC beam resting on an elastic foundation is given by $\bar{u} = \frac{E_p u 100 h^3}{q_0 L^4}(0, \frac{L}{2})$.

These parameters serve as crucial factors influencing the structural response and deformation characteristics of the beam. The considered beam patterns include UD (Unidirectional), FG-O and FG-X. These patterns represent different CNT distributions within the beam, impacting its mechanical properties and deformation behavior. It's noted that the UD, FG-O, and FG-X beam patterns feature antisymmetrical CNT distributions, resulting in zero non-dimensional axial displacements at the midplane of the FG-CNTRC beams resting on the Pasternak elastic foundation. This characteristic is evident from the figure, indicating a balanced distribution of CNTs along the thickness of the beam. However, the FG-O beam distribution exhibits the highest values of dimensionless axial displacements, particularly noticeable at the top edge.

This observation suggests that the FG-O configuration, despite its symmetrical distribution of CNTs, experiences greater deformation under the applied sinusoidal and uniformly distributed load compared to the other patterns considered. Furthermore, an increase in the span-to-thickness ratio leads to a proportional increase in dimensionless axial displacement. This relationship indicates that as the beam becomes longer relative to its thickness, it becomes more susceptible to deformation under the applied load. This phenomenon is consistent with structural mechanics principles, where higher aspect ratios typically result in increased flexibility and deformation.

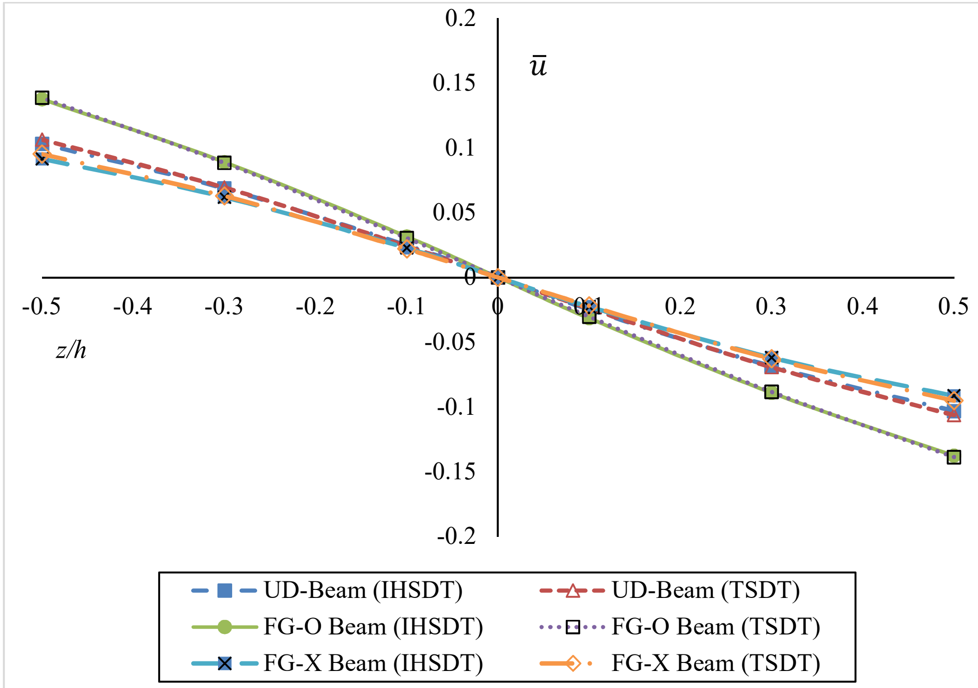

(a)

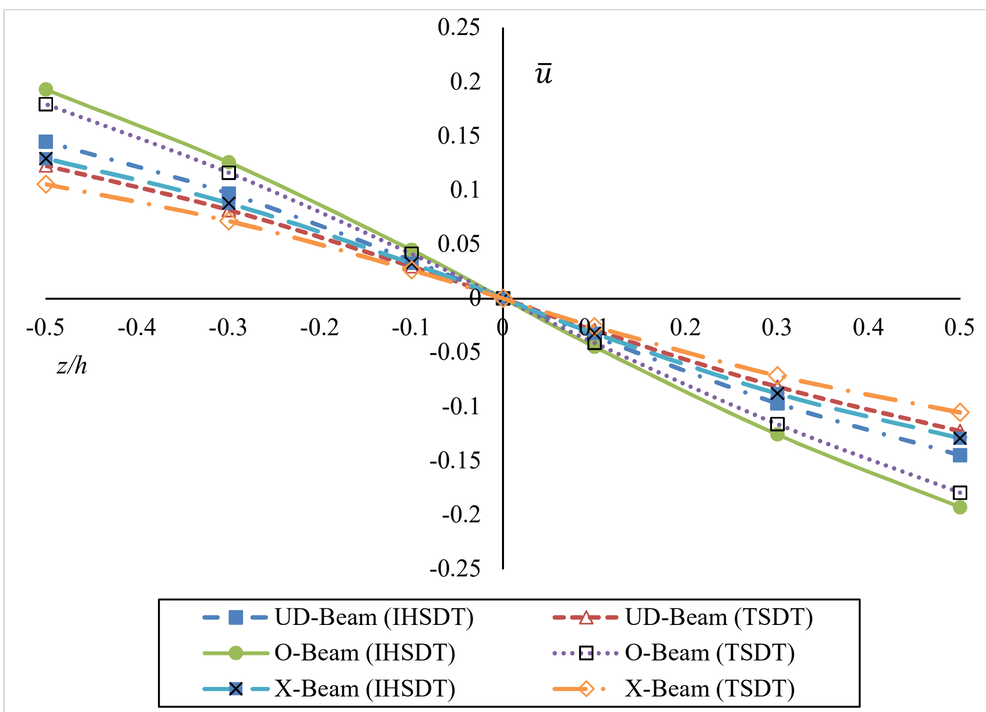

(b)

Figure 4.5. Variation of dimensionless axial deformation of FG-CNTRC beam with an elastic foundation under (a) sinusoidal load and (b) UDL with IHSDT and TSDT (L/h = 10; V_{cnt}^{*} = 0.12; β_w= 0.1, β_s = 0.02)

4.4.1.4 Effect of spring constants on the dimensionless deflection of CNT-Reinforced beam on the Pasternak foundation

In **Figure 4.6**, the researchers analyze the maximum non-dimensional transverse deflection of the FG-X beam under various spring constant parameters. The figure shows the effect of spring constants on the dimensionless deflection of FG-X CNTRC Beam on Pasternak foundation under (a) sinusoidal load and (b) UDL with IHSDT and TSDT. This mathematical approach offers valuable insights into the behavior of the beam, particularly under different foundation stiffness conditions. For this study, a specific span-to-thickness ratio (*L/h*) of 10 is considered, and the composite material includes Carbon Nanotubes (CNTs) with a volume fraction of 0.12. The non-dimensional parameter for calculating the dimensionless transverse displacements of a simply supported CNTRC beam resting on an elastic foundation is given by $\bar{w} = \frac{E_p w 100 h^3}{q_0 L^4}\left(\frac{L}{2}\right)$.

The figure demonstrates a clear trend: as the spring constant parameters increase, there is a nearly linear reduction in the transverse displacements of the FG-X CNTRC beam. This relationship indicates that enhancing the support provided by the elastic foundation, represented by higher spring constant values, leads to a significant decrease in the transverse deflection of the beam. The observed reduction in transverse displacements suggests that a stiffer foundation, indicated by higher spring constant parameters, offers more substantial support to the beam. The figure demonstrates a clear trend: as the spring constant parameters increase, there is a nearly linear reduction in the transverse displacements of the FG-X CNTRC beam. This relationship indicates that enhancing the support provided by the elastic foundation, represented by higher spring constant values, leads to a significant decrease in the transverse deflection of the beam. The observed reduction in transverse displacements suggests that a stiffer foundation, indicated by higher spring constant parameters, offers more substantial support to the beam.

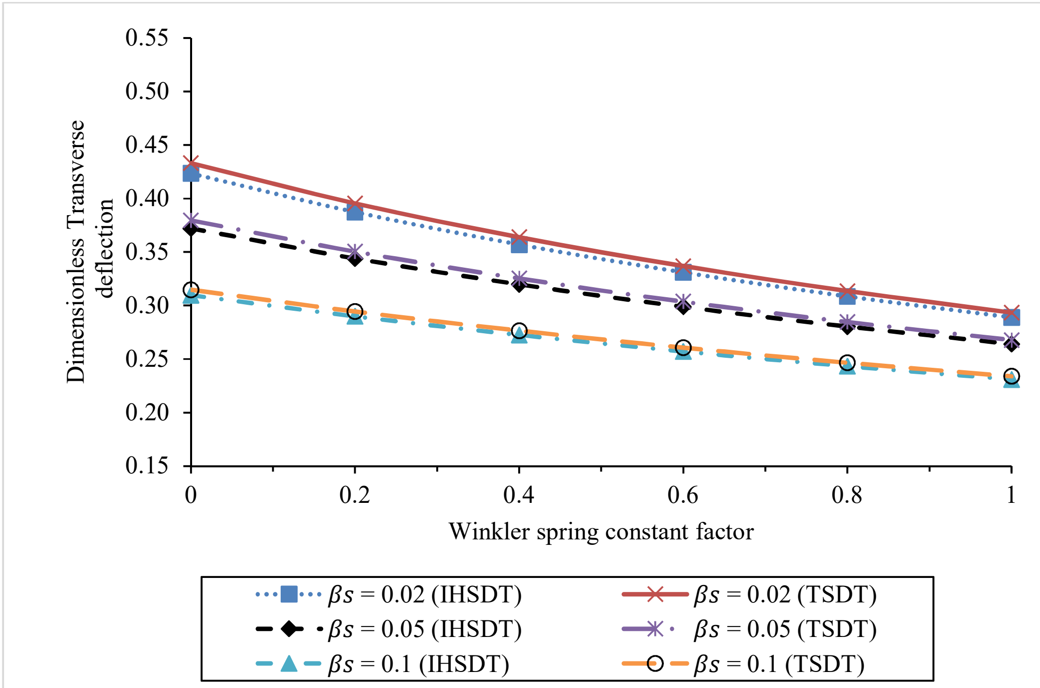

(a)

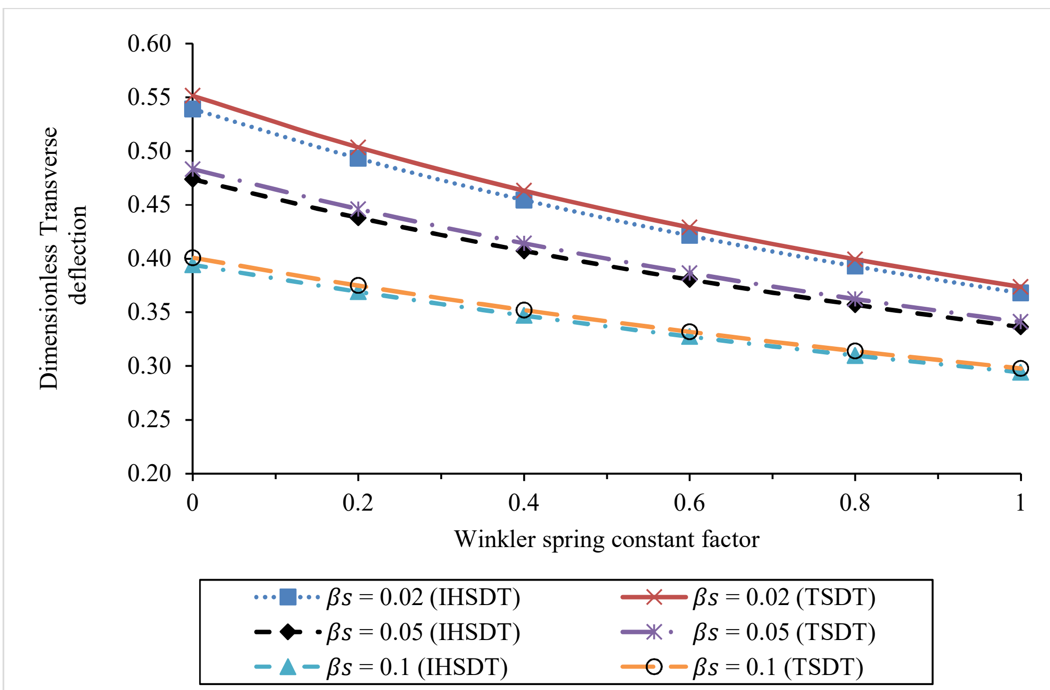

(b)

Figure 4.6. Effect of spring constants on the dimensionless deflection of FG-X CNTRC Beam on Pasternak foundation under (a) sinusoidal load and (b) UDL with IHSDT and TSDT (L/h = 10; V_{cnt}^{*} = 0.12)

As a result, the beam experiences less deflection under the applied loads. This finding is crucial in practical applications because it underscores the importance of adjusting the stiffness of the foundation to control and minimize deformations in composite structures, ensuring their stability and structural integrity.

Figure 4.7 illustrates the effects of varying the Winkler spring and shear layer constant parameters on the dimensionless transverse deflection of an FG-CNTRC beam with an elastic foundation under (a) sinusoidal load and (b) UDL with IHSDT and TSDT.The analysis focuses on the FG-X reinforcement distribution of CNTs along the depth of the beam, with a span-to-thickness ratio (L/h) of 10 and a CNT volume fraction of 0.17.

The figure shows that as the values of the Winkler spring constant and shear layer constant parameters increase, the dimensionless transverse displacement decreases. This indicates that a stiffer foundation, characterized by higher spring and shear layer constants, provides better support and reduces deflection under load. Notably, the dimensionless transverse displacement is more significantly influenced by the shear layer constant parameter than by the Winkler spring constant parameter. An increase in the shear layer constant parameter results in a greater reduction in dimensionless transverse displacement compared to the same increase in the Winkler spring constant parameter.

This difference in impact can be attributed to the nature of the shear layer's support. The shear layer provides additional lateral stiffness, which more effectively resists the transverse load and minimizes deflection. In contrast, the Winkler spring primarily provides vertical support, which, while still beneficial, does not reduce deflection as substantially as the lateral stiffness provided by the shear layer.

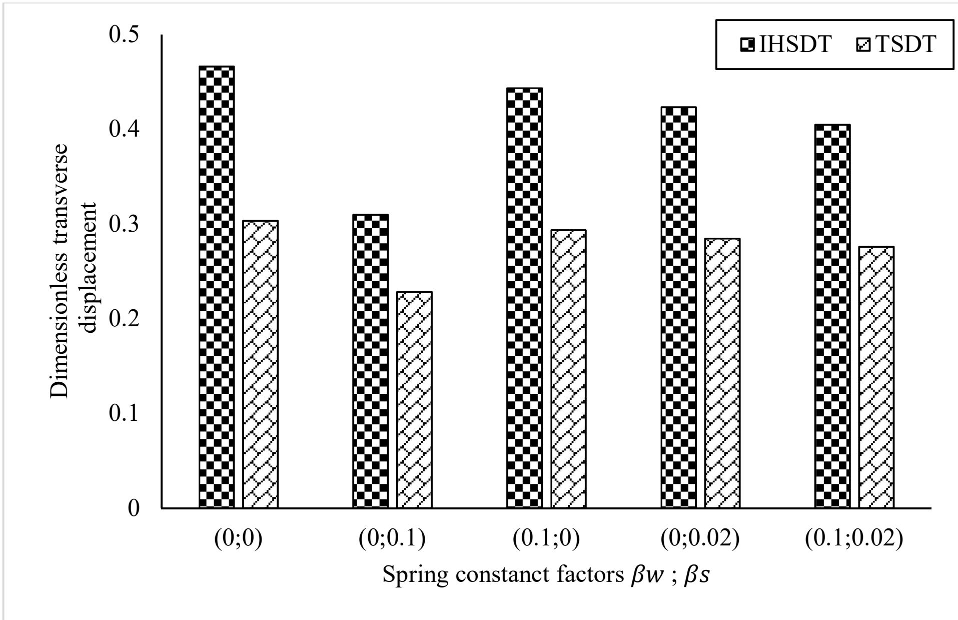

(a)

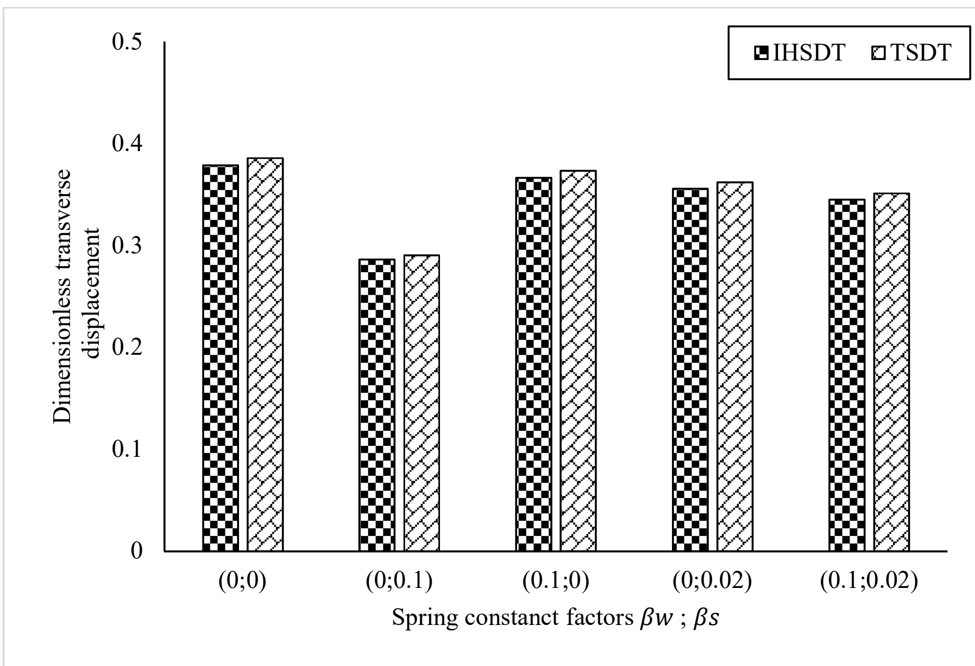

(b)

Figure 4.7. Effect of spring constant parameters on the dimensionless transverse displacement of the FG-CNTRC beam with an elastic foundation under (a) sinusoidal load and (b) UDL with IHSDT and TSDT

4.4.1.5 Effect of CNT distribution on the dimensionless deflection of CNT-Reinforced beam on the Pasternak foundation

Figure 4.8 illustrates the impact of different CNT reinforcement distribution patterns along the thickness of the FG-CNTRC beam on its dimensionless transverse deflection when supported by Pasternak elastic foundation under (a) sinusoidal load and (b) UDL with IHSDT and TSDT. For this analysis, a volume fraction of 0.12, a span-to-thickness ratio (*L/h*) of 10, and Winkler spring and shear layer constants of 0.1 and 0.02, respectively, are used. The different CNT reinforcement distribution patterns considered are UD (Uniform Distribution), FG-X, FG-O, and FG-V.

From the figure, it is evident that the FG-X reinforcement distribution of CNTs across the thickness of the beam offers the greatest resistance to the transverse load "q". This distribution results in the least dimensionless transverse deflection, indicating that the FG-X pattern is highly effective in minimizing deflection and enhancing the load-bearing capacity of the beam. In contrast, the FG-O reinforcement distribution pattern of CNTs demonstrates the opposite behavior compared to the FG-X pattern. The FG-O pattern results in the maximum dimensionless transverse deflection, indicating the least resistance to the transverse load "q". This suggests that the FG-O distribution is less effective in managing the load, leading to greater deflections under the same loading conditions. The differences in performance between these reinforcement patterns can be attributed to the specific configuration and orientation of CNTs within the composite material. The FG-X distribution appears to optimize the mechanical properties and load distribution more effectively, thereby enhancing the structural performance of the beam. On the other hand, the FG-O distribution does not distribute the stresses as efficiently, resulting in higher deflections.

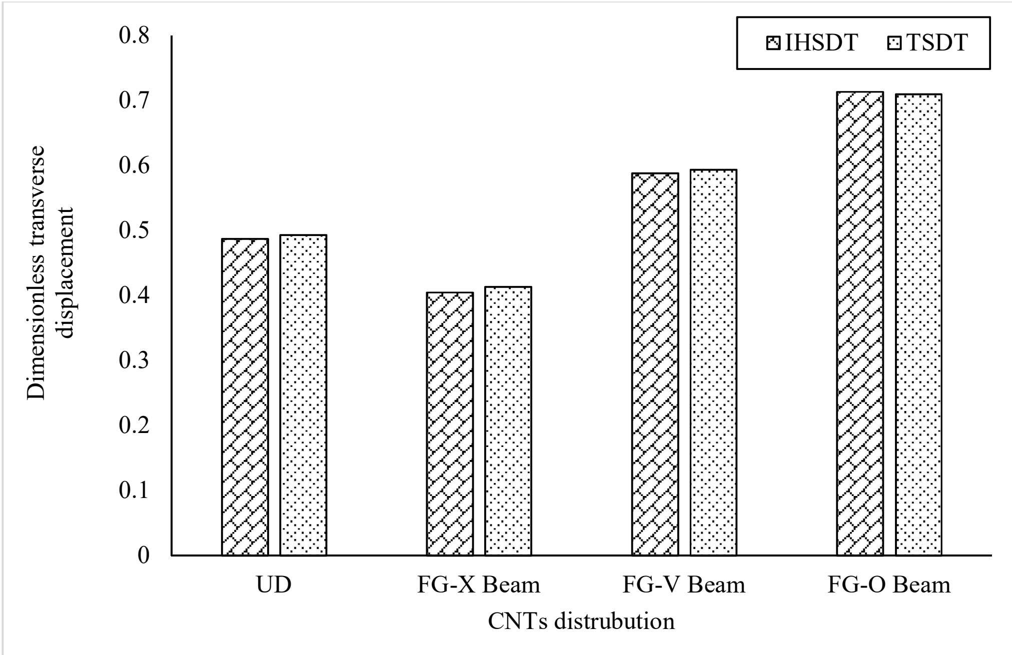

(a)

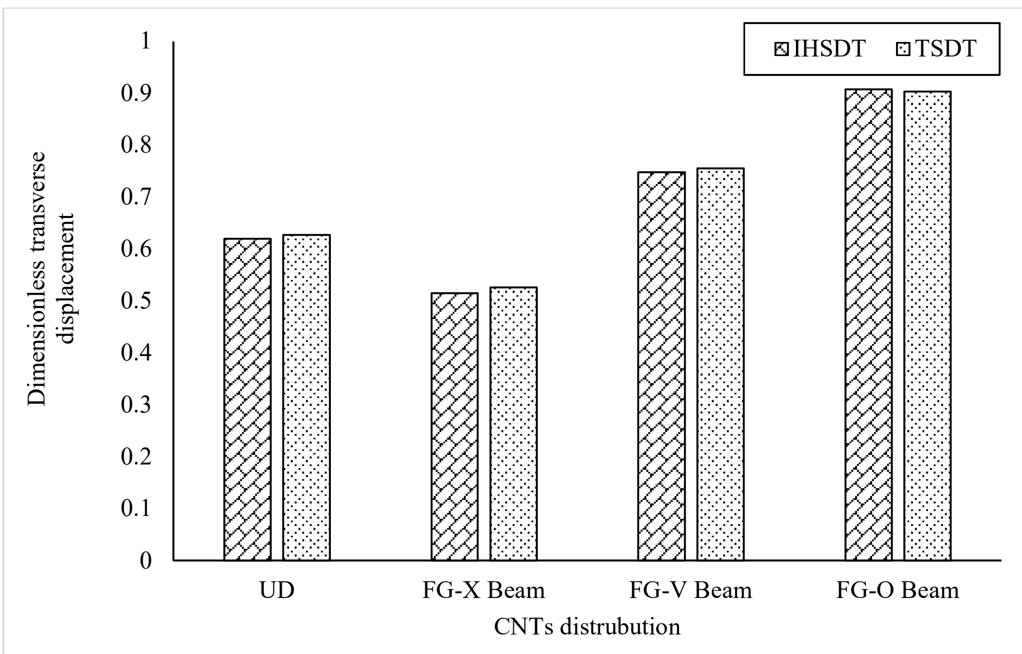

(b)

Figure 4.8. Effect of CNT distribution on the dimensionless deflection of FG-CNTRC Beam on Pasternak foundation under (a) sinusoidal load and (b) UDL with IHSDT and TSDT (*L/h* = 10; V_{cnt}^{*} = 0.12)

4.4.1.6 Stress analysis of the composite beam resting on the Pasternak elastic foundation reinforced with carbon nanotubes

This section covers the stress analysis of a carbon nanotube reinforced composite beam resting on a Pasternak elastic foundation under various parametric conditions. The stress distribution of the beam is analyzed analytically. A detailed examination is conducted on the impact of varying span thickness ratios, carbon nanotube (CNT) volume fraction, and CNT distribution on the stress distribution. Four different CNT reinforcement distribution types are considered for the analysis. These include three different forms of functionally graded (FG) CNT distribution FG-O, FG-X, and FG-V as well as uniformly distributed (UD) CNTs.

The aim is to find the optimal configuration for the reinforcement distribution to enhance the stress distribution response of the functionally graded carbon nanotube (CNT) reinforced composite beam resting on the Pasternak elastic foundation. The trigonometric shear deformation theory, which includes secant and inverse sine functions, forms the foundation for the analytical analysis. This method enables a more accurate depiction of the behaviour of the beam under various loading scenarios. Examining the stress distribution under different parametric conditions can enhance the design and performance of carbon nanotube reinforced composite beams with elastic foundations.

4.4.1.6.1 Normal stress distribution in a composite beam resting on the Pasternak elastic foundation reinforced with carbon nanotubes

Examining the fluctuation of the dimensionless axial stress in a Carbon Nanotube Reinforced Composite (CNTRC) beam resting on a Pasternak elastic foundation under sinusoidal load and Uniformly Distributed Loading conditions can provide important information about the structural response of the material. This investigation examines the effects of different loading conditions on the axial stress along the length of the beam.

Understanding the variance in dimensionless axial stress helps identify critical points for potential failure, assess the behaviour of the material, and refine the design of CNTRC beams for improved performance and durability.

Figure 4.9 shows the variation of dimensionless axial stress in a Carbon Nanotube Reinforced Composite (CNTRC) beam resting on the Pasternak elastic foundation under Uniformly Distributed Loading and sinusoidal loading conditions. The figure shows the variation of non-dimensional axial stress of the CNTRC beam with an elastic foundation under (a) sinusoidal load and (b) UDL with inverse hyperbolic shear deformation theory and trigonometric shear deformation theory. The analysis uses a carbon nanotube volume fraction (V_{cnt}^{*}) of 0.12 and a span-to-thickness ratio (L/h) of 10. The non-dimensional parameter for calculating the dimensionless axial stress of a simply supported CNTRC beam resting on an elastic foundation is given by $\bar{\sigma}_{xx} = \frac{h}{q_0 L} \sigma_{xx}(\frac{L}{2}, \frac{h}{2})$.

The figure illustrates the symmetrical distributions of CNTs before and after the CNTRC mid-plane of the beam in the UD (Uniform Distribution), FG-X, and FG-O beams. This symmetry suggests that the characteristics of the material and the CNT reinforcement are mirrored along the mid-plane, promoting balanced structural behavior under load. An important finding from the figure is that there are no dimensionless normal strains at the CNTRC mid-plane of the beam. This indicates an equilibrium point where the tensile and compressive stresses balance each other out. Due to symmetric loading and material distribution, the zero stress value at the mid-plane ensures that there is no net normal stress at this central location.

Dimensionless normal stresses fluctuate before and after the mid-plane, exhibiting identical magnitudes but opposite characteristics. This indicates that on both sides of the mid-plane, the normal stresses have the same absolute values but different signs. For example, compressive stress occurs below the mid-plane while tensile stress occurs above it.

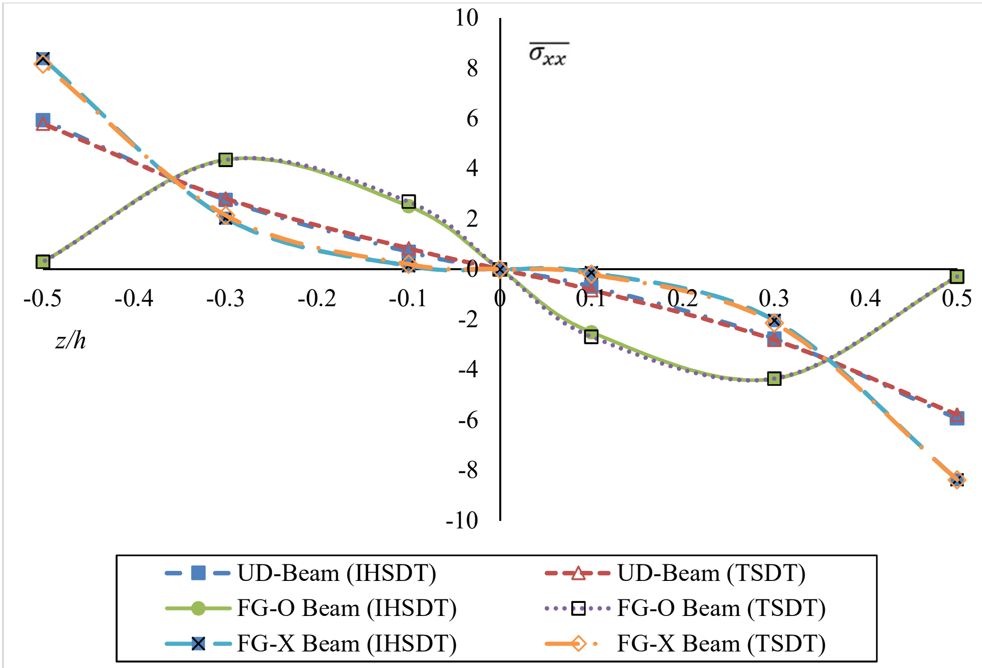

(a)

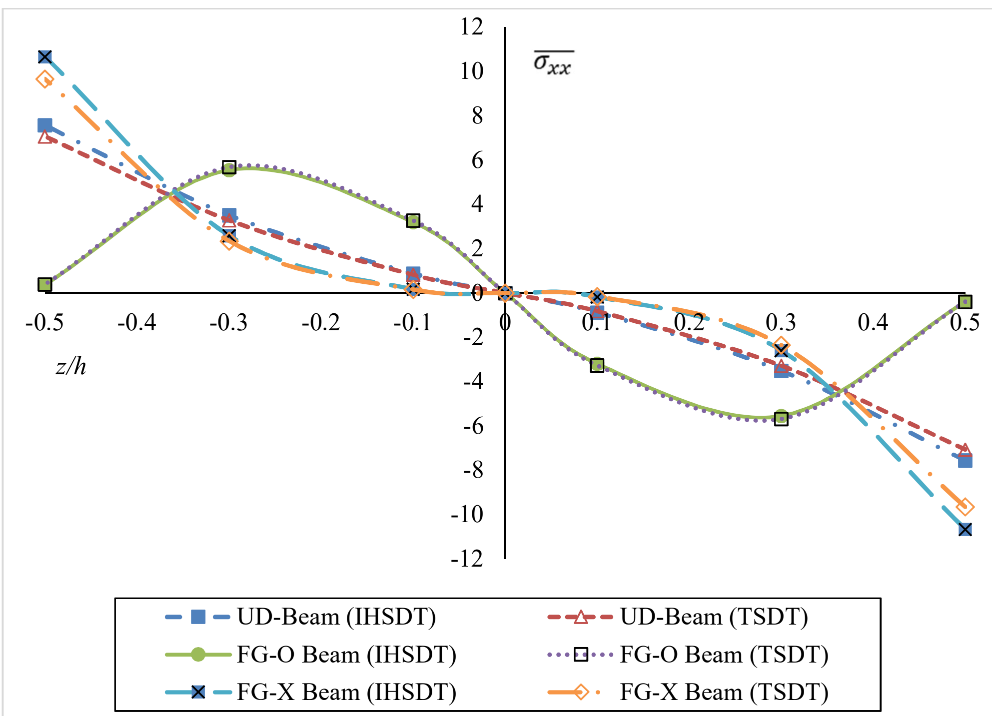

(b)

Figure 4.9. Variation of dimensionless axial stress of CNTRC beam with an elastic foundation under (a) sinusoidal load and (b) UDL with IHSDT and TSDT (*L/h* = 10; V_{cnt}^{*} = 0.12; β_w= 0.1, β_s = 0.02)

The FG-O beam distribution yields the lowest values of normal stress when the variation of dimensionless normal stresses at the upper edge of the beam is examined. This result is notable because it implies that the FG-O beam arrangement is highly effective at reducing normal stresses at the extreme fiber of the beam, where stresses typically reach their maximum values. The decreased normal stress in the FG-O beam structure may be attributed to the specific configuration and orientation of CNTs, which enhance the load-carrying capacity and more effectively distribute the stresses over the cross-section of the beam.

4.4.2. Buckling analysis of FG-CNT reinforced beams on the Pasternak elastic foundation

In this section, the buckling analysis of the CNTRC (Carbon Nanotube Reinforced Composite) beam with the Pasternak elastic foundation under uniaxial compressive loads is discussed in detail. The analysis considers various parametric conditions, including different volume fractions of CNTs, different CNT distribution patterns, and different spring constant factors. The study examines how varying the volume fraction of CNTs affects the buckling behavior of the CNTRC beam. Higher CNT content generally enhances the stiffness and strength of the composite material, potentially increasing the buckling resistance. Different patterns of CNT reinforcement distribution within the beam are analyzed. The spring constant factors in Pasternak elastic foundation model, which include the Winkler spring constant and the shear layer constant, are varied to study their impact on buckling behavior.

4.4.2.1 Buckling analysis of FG-CNT reinforced beams on Pasternak elastic foundation under uniaxial compression

A crucial factor in structural engineering is the critical buckling load, which is the highest load a beam can support before buckling causes it to become unstable and potentially fail. The main topic of discussion is the critical buckling load of simply supported carbon nanotube reinforced composite (CNTRC) beams resting on Pasternak elastic foundation under uniaxial compressive load with an *L/h* ratio of 15, considering various carbon nanotube (CNT) volume fractions, as shown in **Table 4.13**.

The table also provides a comparative study of the critical buckling load for CNTRC beams with different CNT distribution patterns. The governing equations for the buckling analysis are developed using the trigonometric shear deformation theory, which includes secant and inverse sine functions. Navior's solution technique is employed in the analytical approach to solve these equations. The non-dimensional parameter for calculating the critical buckling load of a simply supported CNTRC beam resting on an elastic foundation is given by $\bar{N}_{x0} = \frac{N_{cr}}{A_{110}}$.

The critical buckling load for each of the four types of CNTRC beams UD (uniform distribution), FG-O, FG-X, and FG-V is compared in this table. These patterns likely relate to the arrangement of carbon nanotubes within the composite material, significantly impacting the mechanical characteristics and load-bearing capability of the beam. The analysis presents the critical buckling load for two distinct shear deformation theories and compares it with the findings of Yas and Samadi (2012), which are based on Timoshenko beam theory (TBT). The table indicates a good agreement between the presented results and those found in the literature. The results of evaluating the buckling load using various theoretical models are also compared in the table. This comparison is necessary to confirm the reliability and accuracy of the employed analytical techniques. As the volume fraction (V_{cnt}^{*}) of CNTs increases, and the critical buckling load also grows. This pattern highlights the role of carbon nanotubes (CNTs) in strengthening the composite material by enhancing its stiffness and strength, both of which are essential for preventing buckling. The table shows that under uniaxial compressive load, the non-dimensional critical buckling load increases in proportion to the volume fraction of CNTs in a CNTRC beam. Similarly, it is found that with an unsymmetrical FG-V distribution, an increase in the volume fraction of CNTs in a CNTRC beam results in an increase in the non-dimensional critical buckling load under uniaxial compressive force. The FG-O distribution pattern of reinforcing CNTs across the thickness of the CNTRC beam produces the lowest resistance to the non-dimensional critical buckling load under uniaxial compressive force. In contrast, the FG-X reinforcement distribution pattern provides the highest resistance to the non-dimensional critical buckling load under uniaxial compressive stress across the thickness of the CNTRC beam.

Table 4.13 Critical buckling load of FG-CNTRC beams (L/h =15; $\beta_w = 0.1,\ \beta_s$= 0.02)

V^*_{cnt}	Source	UD-Beam	FG V-Beam	FG O-Beam	FG X-Beam
	Present (IHSDT)	0.1230	0.0990	0.0830	0.1540
0.12	**Present (TSDT)**	0.1228	0.0995	0.0840	0.1526
	TBT*	0.1280	0.1220	0.0880	0.1580
	Present (IHSDT)	0.1720	0.1340	0.1100	0.2200
0.17	**Present (TSDT)**	0.1715	0.1343	0.1109	0.2185
	TBT*	0.1800	0.1700	0.1170	0.2300
	Present (IHSDT)	0.2400	0.1870	0.1540	0.2980
0.28	**Present (TSDT)**	0.2389	0.1871	0.1547	0.2964
	TBT*	0.2510	0.2390	0.1630	0.3190

*Yas and Samadi (2012),

The results of various deformation theories provided by Wattanasakulpong and Ungbhakorn (2013), as well as Yas and Samadi, have been compared with the critical buckling load results for a Carbon Nanotube Reinforced Composite (CNTRC) beam resting on the Pasternak elastic foundation with a volume fraction of 0.12 and a span-to-thickness ratio of 15, as shown in **Table 4.14**. The results of the current study are in good agreement with those of the results obtained from different deformation theories, demonstrating the reliability and accuracy of the current analysis. The FG-V Beam exhibits special stretching-bending coupling features because of its inherent asymmetry. Due to this coupling effect, the V-Beam experiences bending moments and deflections in addition to direct axial compression when subjected to compressive loads. This phenomenon occurs because of the differential stiffness caused by the uneven distribution of CNTs over the cross-section of the beam, leading to simultaneous stretching and bending under compression. As a result, the FG-V Beam avoids the typical bifurcation-type buckling, which would cause the beam to abruptly change its deformation pattern at the critical load. Instead, the response of the FG-V Beam to compressive stress is more complex, involving a gradual increase in bending moments and deflections. Among the compared beam types (FG-X Beam, UD-Beam, and FG-O Beam), the FG-X Beam is found to be the strongest in the current analysis. Due to its exceptional stability and resistance to buckling under compressive stresses, the FG-X Beam is capable of supporting the maximum buckling load. The optimal orientation and distribution of CNTs in the FG-X Beam, which enhances its stiffness and load-bearing capacity, are likely the reasons for its superior performance.

Table 4.14 Nondimensional buckling load for different distributions of FG-CNTRC beam ($V_{cnt}^{*} = 0.12$; $L/h = 15$; $\beta_w = 0.1$, β_s= 0.02)

Source	UD-Beam	FG-O Beam	FG-X Beam
Present (IHSDT)	0.1235	0.0837	0.1543
Present (TSDT)	0.1228	0.0840	0.1526
TSDT*	0.1286	0.0878	0.1590
ESDT*	0.1286	0.0875	0.1596
HSDT*	0.1286	0.0878	0.1590
TrSDT*	0.1287	0.0876	0.1592
FSDT*	0.1333	0.0905	0.1668
TBT**	0.1287	0.0889	0.1590
TrBT***	0.1286	0.0876	0.1592

*Wattanasakulpong and Ungbhakorn (2013), **Yas and Samadi (2012)

The analysis reveals significant information about the critical buckling behavior of functionally graded Carbon Nanotube Reinforced Composite (FG-CNTRC) beams resting on the Pasternak elastic foundation under varied span-to-thickness (*L/h*) ratios and CNT volume fractions. The non-dimensional parameter for calculating the dimensionless critical buckling load of a simply supported CNTRC beam resting on an elastic foundation is given by $\overline{N}_{x0} = \frac{N_{cr}}{A_{110}}$. The findings, depicted in **Figure 4.10**, demonstrate how the stability and load-bearing capability of the beam are affected by the distribution of CNTs across its cross-section. **Figure 4.10** illustrates different configurations of CNT reinforcement across the cross-section of various FG-CNTRC beams. The analysis compares four distinct distribution patterns: FG-O, FG-X, FG-V, and UD (Uniform Distribution). Among all distribution types, the FG-X pattern achieves the highest critical buckling load, highlighting a significant finding. This suggests that the FG-X arrangement is the optimal choice for enhancing the stability of the beam under compressive stresses. Additionally, increasing the volume fraction of CNTs raises the critical buckling load. This pattern illustrates the reinforcing effect of carbon nanotubes (CNTs), where higher concentrations of CNTs result in increased stiffness and consequently greater resistance to buckling.

The critical buckling load is depicted in relation to the *L/h* ratio for the following CNT distribution patterns: UD, FG-O, FG-X, and FG-V. The critical buckling load decreases as the *L/h* ratio increases. This occurs because a beam with a larger *L/h* ratio is more prone to buckling under compressive pressure due to its slenderness. Thinner beams are less stable and have lower stiffness, resulting in lower critical buckling loads. The graph indicates a significant change in the critical buckling load when the *L/h* ratio ranges between 15 and 30. **Figure 4.11** presents the non-dimensional critical buckling loads of the FG-X Beam under various spring constant parameters, using the trigonometric shear deformation theory, which includes IHSDT and TSDT to examine the influence of these parameters on the buckling behavior. In this analysis, the span-to-thickness ratio (*L/h*) is set to 10, and the volume fraction of CNTs (V_{cnt}^{*}) is 0.12.

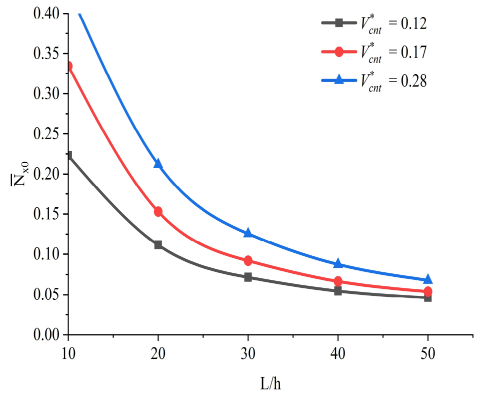

(a)

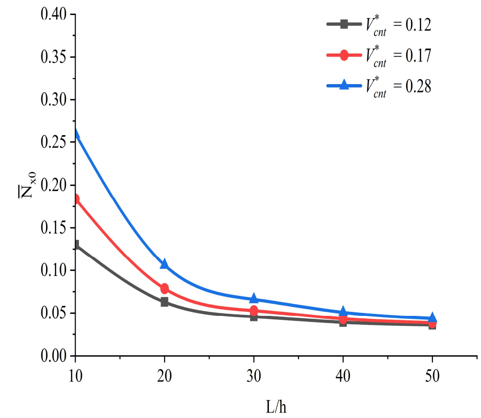

(b)

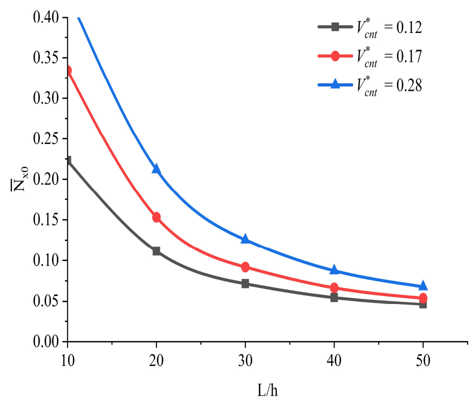

(c)

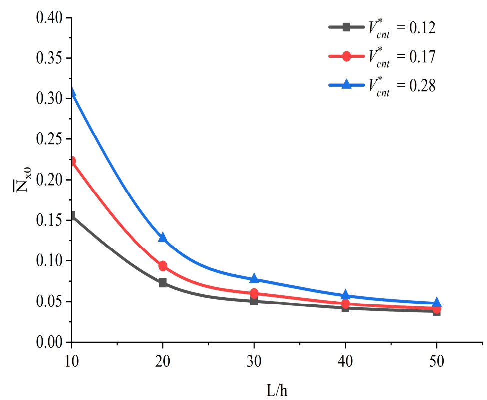

(d)

Figure 4.10. Dimensionless critical buckling load of (a) UD- Beam, (b) FG-O Beam, (c) FG-X Beam, and (d) FG-V Beam resting on elastic foundation with varying *L/h* ratios ($\beta_w = 0.1,\ \beta_s = 0.02$)

The figure illustrates a clear linear relationship between the dimensionless buckling loads and the spring constant parameter. As the Winkler spring constant parameter and shear layer constant factor increase, there is a corresponding increase in the buckling load of the FG-X Beam. The Winkler spring constant parameter enhances the support provided by the foundation, while the shear layer constant factor reinforces the beam against lateral deflections. Together, these factors contribute to an overall enhancement in the resistance to buckling of the beam.

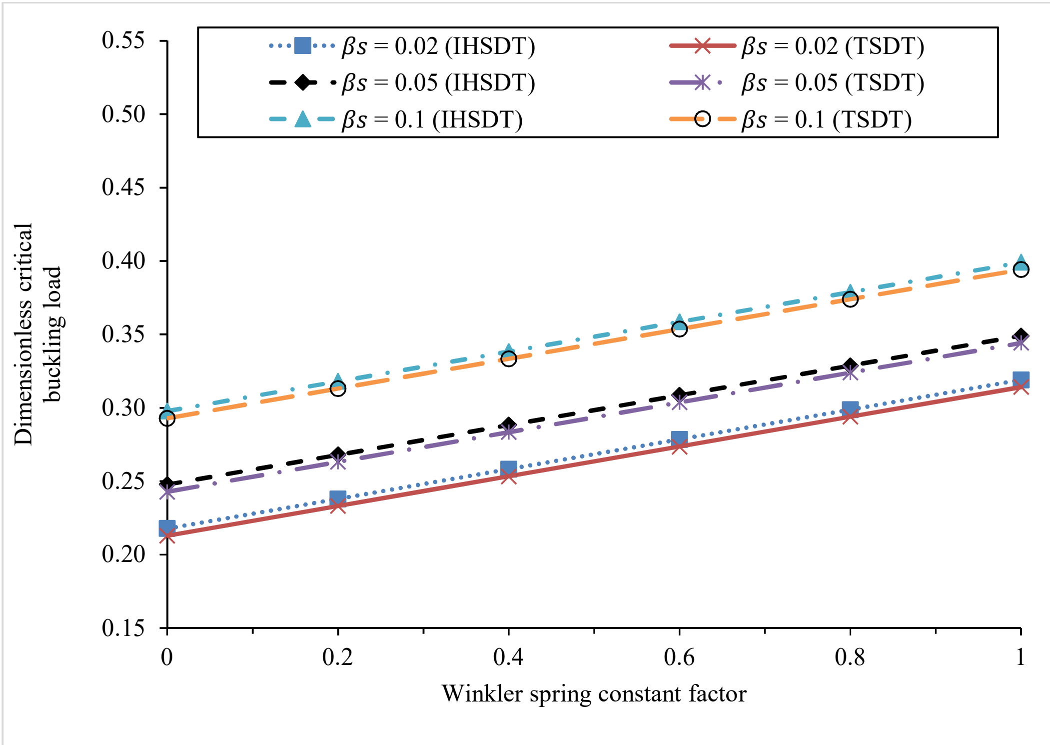

Figure 4.11. Effect of various spring constant parameters on the dimensionless critical buckling load of an FG-X Beam with an elastic foundation with IHSDT and TSDT (*L/h* = 10; V_{cnt}^{*} = 0.12)

Figure 4.12 depicts the influence of the Winkler modulus parameter on the critical buckling loads of CNTRC beams with an elastic foundation by using a non-polynomial shear deformation theory i.e., IHSDT and TSDT, specifically focusing on an *L/h* ratio of 10, shear layer spring constants (β_s) of 0, and a CNT volume fraction (V_{cnt}^{*}) of 0.12. This graph visually illustrates how varying the Winkler modulus parameter affects the critical buckling loads of CNTRC beams, providing valuable insights into their structural behavior under different modulus values.

The figure demonstrates that the FG-X Beam exhibits a higher critical buckling load as the Winkler modulus parameter increases. This outcome can be attributed to several factors: the concentrated reinforcement of carbon nanotubes (CNTs) in the FG-X Beam configuration, the enhanced stiffness resulting from the higher modulus, optimized load transfer capabilities, and improved overall structural integrity. These aspects collectively contribute to making the FG-X Beam more resistant to buckling compared to beams with different distributions of CNTs. Moreover, the graph shows a linear relationship where the critical buckling loads increase as the Winkler modulus parameter rises. This linear trend indicates that increasing the modulus enhances the ability of the beam to withstand buckling under compressive loads. The inclusion of higher spring constant factors further reinforces this effect by providing additional support against lateral deflections, thereby contributing to the overall increase in buckling load.

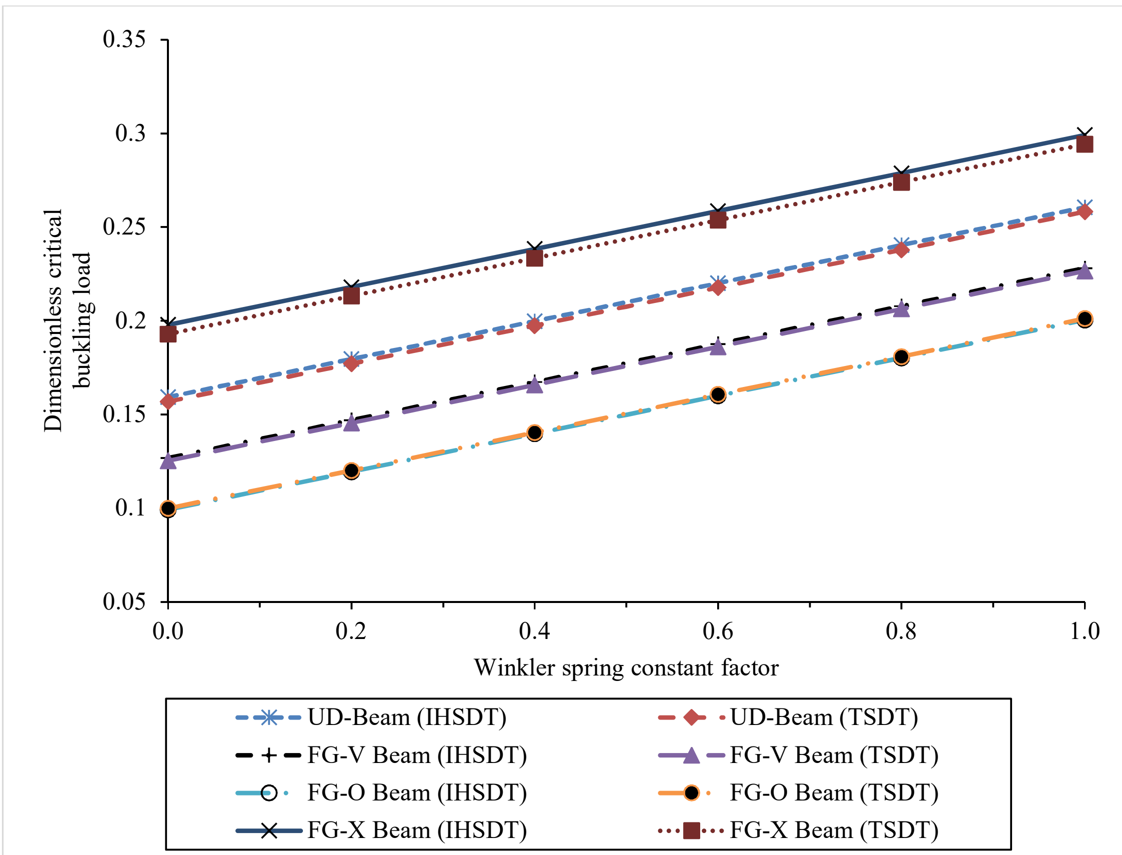

Figure 4.12. Effect of Winkler modulus parameters on the dimensionless critical buckling load of FG-CNTRC Beam with an elastic foundation with IHSDT and TSDT (L/h = 10; V_{cnt}^{*} = 0.12)

4.4.3 Free vibration analysis of FG-CNT reinforced beams on the Pasternak elastic foundation

This section analyzes the impacts of different parameters on the non-dimensional natural frequency, including CNT volume fractions, length-to-thickness ratios, and CNT distribution patterns, to explore the dynamic behavior of a simply supported carbon nanotube reinforced composite (CNTRC) beam resting on the Pasternak elastic foundation. The governing equations for this dynamic study are derived using trigonometric shear deformation theory, incorporating secant and inverse sine functions. The dynamic behavior of the CNTRC beam under these conditions is analyzed analytically using Navier's solution technique.

The non-dimensional natural frequency is calculated using a span-to-thickness ratio of 15, considering three CNT volume fractions (V_{cnt}^{*} = 0.12, 0.17, and 0.28), and varying CNT distribution patterns across the beam. The non-dimensional parameter for calculating the dimensionless natural frequency of CNTRC beam resting on an elastic foundation is given by $\bar{\omega} = \omega L\sqrt{\frac{I_{00}}{A_{110}}}$. The obtained natural frequency results are compared with those from previous studies, such as Timoshenko Three-beam Theory (TBT) by Yas and Samadi (2012) as shown in **Table 4.15**. These comparisons utilize trigonometric shear deformation theory based on secant and inverse sine functions. The comparison reveals a good agreement between the provided results and the existing data.

In the CNTRC beam resting on the Pasternak elastic foundation, the non-dimensional natural frequency is found to be maximum for the FG-X Beam configuration and lowest for the FG-O Beam configuration, given a specific length-to-thickness ratio and CNT volume fractions. Additionally, for a particular volume fraction of CNTs and a specific length-to-thickness ratio, the highest non-dimensional natural frequency is observed in the FG-X Beam, followed sequentially by the UD (uniformly distributed) Beam, the FG-V Beam, and the FG-

O Beam. This highlights the significant impact of CNT distribution patterns on the dynamic characteristics of the CNTRC beam with an elastic foundation, with the FG-X Beam configuration providing superior reinforcement in enhancing the natural frequency.

Table 4.15 Dimensionless natural Frequency of FG-CNTRC beam resting on an elastic foundation (L/h = 15; $\beta_w = 0.1$, β_s= 0.02)

V^*_{cnt}	Source	UD-Beam	FG-V Beam	FG-O Beam	FG-X Beam
	Present (IHSDT)	1.0940	0.9830	0.9010	1.2230
0.12	**Present (TSDT)**	1.0913	0.9819	0.9024	1.2163
	TBT*	1.1140	1.0880	0.9250	1.2380
	Present (IHSDT)	1.2870	1.1380	1.0310	1.4550
0.17	**Present (TSDT)**	1.2843	1.1360	1.0328	1.4493
	TBT	1.3140	1.2790	1.0610	1.4830
	Present (IHSDT)	1.5070	1.3310	1.2080	1.6760
0.28	**Present (TSDT)**	1.5015	1.3282	1.2083	1.6723
	TBT	1.5350	1.5000	1.2400	1.7330

*Yas and Samadi (2012)

The dynamic behavior of a carbon nanotube reinforced composite (CNTRC) beam resting on the Pasternak elastic foundation with simple support is analyzed, considering a specific CNT volume fraction of 0.12 and a span-to-thickness ratio of 15. **Table 4.16** shows the results from various deformation theories and the Timoshenko beam theory (TBT), as given by Wattanasakulpong and Ungbhakorn (2013) and Yas and Samadi (2012) respectively, which are compared to the specific results of the dimensionless natural frequency of the same FG-CNTRC beam with an elastic foundation.

The table illustrates a good agreement between the findings from various deformation theories and those from trigonometric shear deformation theory, which utilizes inverse sine and secant functions. It reveals that the non-dimensional natural frequency is highest for the

FG-X Beam distribution pattern and lowest for the FG-O Beam distribution pattern at a specific length-to-thickness ratio and CNT volume fraction.

Based on free vibration analysis, the FG-X Beam is identified as the strongest configuration, exhibiting the highest non-dimensional natural frequency. This is followed by the UD (uniformly distributed) Beam, the FG-V Beam, and lastly, the FG-O Beam. This indicates the significant impact of the CNT distribution pattern on the dynamic characteristics of the CNTRC beam with an elastic foundation, with the FG-X Beam providing the most effective reinforcement in terms of natural frequency.

Table 4.16 Comparative of non-dimensional natural frequencies for various distributions for CNTRC beam resting on an elastic foundation (L/h = 15; $V_{cnt}^{*} = 0.12$; $\beta_w = 0.1$, β_s= 0.02)

Source	UD-Beam	FG-O Beam	FG-X Beam	FG-V Beam
Present (IHSDT)	1.0944	0.9012	1.2231	0.9838
Present (TSDT)	1.0913	0.9024	1.2163	0.9819
TSDT*	1.1137	0.9198	1.2387	1.0014
ESDT*	1.1147	0.9187	1.2413	1.0020
HSDT*	1.1137	0.9198	1.2387	1.0014
TrSDT*	1.1140	0.9192	1.2397	1.0016
FSDT*	1.1339	0.9339	1.2688	1.0142
TBT**	1.1144	0.9258	1.2386	1.0883
TrBT***	1.1140	0.9192	1.2397	1.0015

*Wattanasakulpong and Ungbhakorn (2013), **Yas and Samadi (2012)

The fundamental frequencies of carbon nanotube reinforced composite (CNTRC) beam resting on an elastic foundation are depicted in **Figure 4.13** across various CNT volume fractions, length-to-thickness ratios, and CNT reinforcement configurations along the cross-section of the beam. The non-dimensional parameter for calculating the dimensionless natural frequency of a simply supported CNTRC beam resting on an elastic foundation is given by $\overline{\omega} = \omega L \sqrt{\frac{I_{00}}{A_{110}}}$. Understanding how these variables influence the dynamic behavior of CNTRC beams with elastic foundations is crucial for their application in engineering structures where vibration performance is critical. This analysis aims to facilitate that understanding. It is evident that the non-dimensional natural frequency of CNTRC beams with elastic foundation is significantly influenced by the length-to-thickness ratio (*L/h*).

The fundamental frequency decreases as the length-to-thickness ratio increases. Longer and thinner beams with larger length-to-thickness ratios exhibit lower vibrational frequencies due to their greater flexibility and reduced stiffness. Analysis of the impact of the CNT volume fraction (V_{cnt}^{*}) reveals that higher CNT content results in an increase in the fundamental frequency of the CNTRC beam. This increase in frequency is attributed to the enhanced stiffness and material qualities provided by carbon nanotubes (CNTs), which strengthen the beam structure and improve its dynamic response. The trends observed in buckling analysis are reflected in the behavior of CNTRC beams under vibrational analysis. Specifically, both buckling load and natural frequency decrease as the span-to-thickness ratio (*L/h*) is increased. Similarly, increasing the CNT volume percentage enhances both buckling resistance and natural frequency.

The outcomes depicted in **Figure 4.13** underscore the significant impact of CNT distribution patterns on the dynamic characteristics of CNTRC beams with elastic foundations. The FG-X Beam configuration develops as the optimal choice for enhancing dynamic performance, as it exhibits the highest efficiency in increasing natural frequencies. In contrast, the FG-O Beam arrangement shows the lowest natural frequencies, despite potentially offering advantages in other mechanical qualities or design considerations. The FG-V Beam provides an intermediate option, while the UD Beam demonstrates balanced performance and serves as a reliable standard.

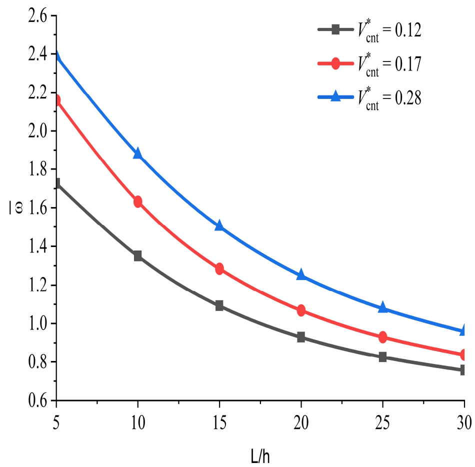

(a)

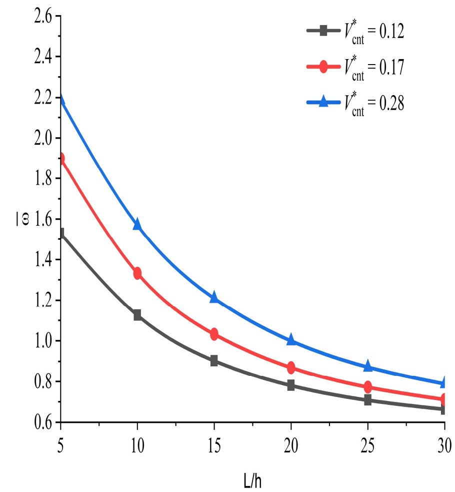

(b)

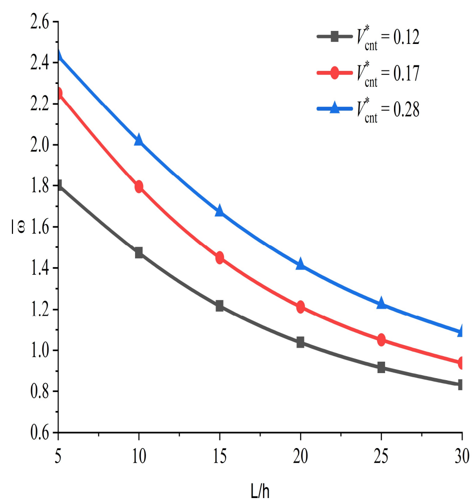

(c)

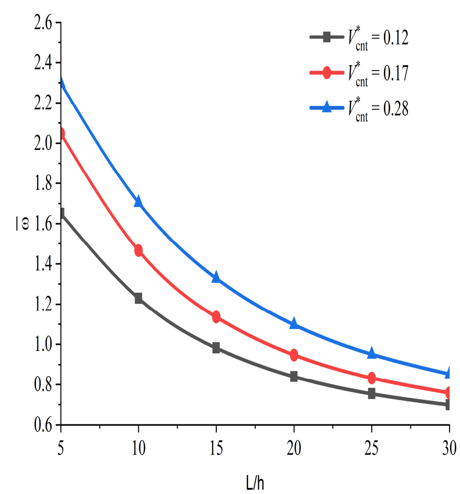

(d)

Figure 4.13. Non-dimensional natural frequencies of (a) UD Beam, (b) FG-O Beam, (c) FG-X Beam, and (d) FG-V Beam resting on elastic foundation with varying *L/h* ratios ($\beta_w =$ 0.1, β_s= 0.02)

In **Figure 4.14**, the dimensionless fundamental frequency of the FG-X Beam is graphically presented with varying spring constant parameters. The analysis employs the trigonometric shear deformation theory, incorporating inverse sine functions (IHSDT) and secant function (TSDT) to investigate how changes in the spring constant parameter influence the fundamental frequency of the FG-X Beam. Specifically, the volume fraction of CNTs is set at 0.12, and the span-to-thickness ratio (*L/h*) is assumed to be 10. From the figure, it is evident that the dimensionless fundamental frequency increases in a linear fashion as the spring constant parameter is incremented.

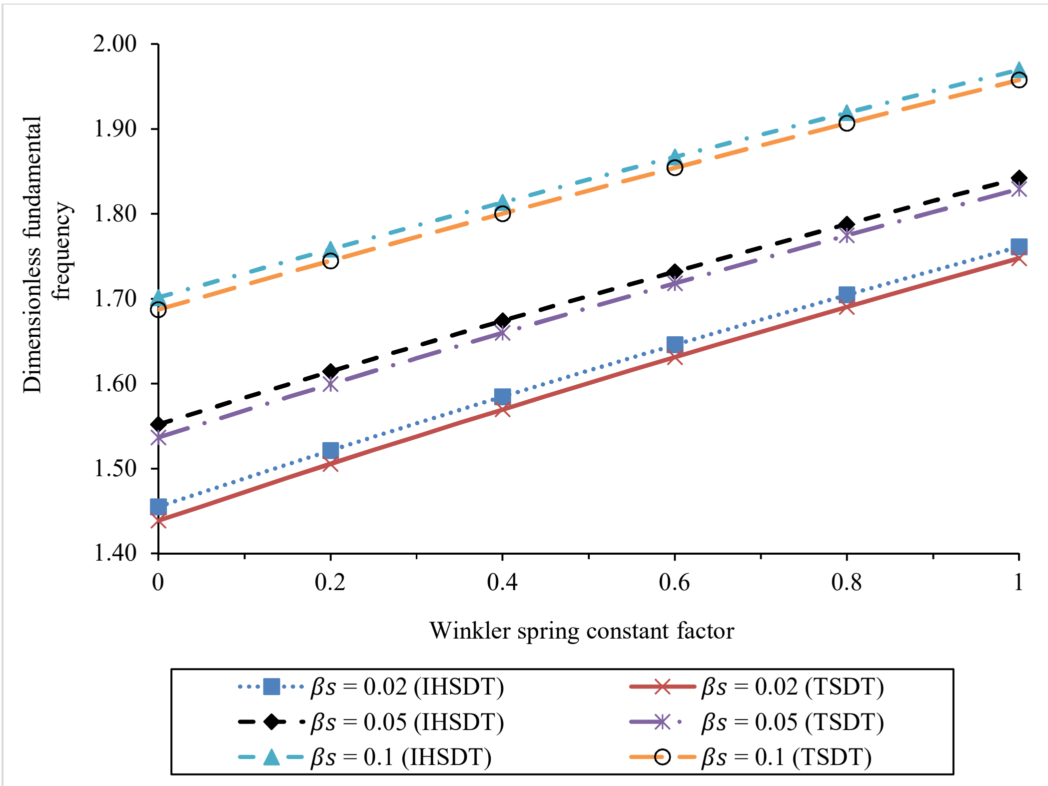

Figure 4.14. Effect of various spring constant parameters on the non-dimensional fundamental frequency of an FG-X Beam resting on a Pasternak elastic foundation with IHSDT and TSDT (*L/h* = 10; V_{cnt}^{*} = 0.12)

This relationship indicates that higher values of the spring constant parameter lead to a higher fundamental frequency of the FG-X Beam. Furthermore, the figure illustrates that enhancing both the Winkler spring constant parameter and the shear layer constant factor concurrently reinforces the beam and improves its resistance to buckling.

The shear layer constant factor primarily strengthens the beam against lateral deflections, whereas the Winkler spring constant parameter enhances the support provided by the foundation. Together, these effects contribute to a linear augmentation in the non-dimensional fundamental frequency of the FG-X Beam.

In **Figure 4.15**, the impact of the Winkler modulus parameter on the fundamental frequencies of CNTRC beams resting on a Pasternak elastic foundation with IHSDT and TSDT is depicted. The analysis focuses on specific conditions: an *L/h* ratio of 10, shear layer spring constants (β_s) set to 0, and a fixed volume fraction of CNTs at 0.12. The graph visually represents how variations in the Winkler modulus parameter influence the fundamental frequencies of CNTRC beams, providing insights into their dynamic response across different values of the Winkler modulus. Notably, the figure demonstrates that as the Winkler modulus parameter increases, the fundamental frequencies of the FG-X Beam also increase. This can be attributed to several factors: concentrated reinforcement, increased stiffness resulting from the higher modulus, optimized load transfer, and improved structural integrity. These qualities collectively contribute to the FG-X Beam exhibiting higher fundamental frequencies compared to other beams with different CNT distribution patterns. Additionally, the graph shows a linear relationship between the fundamental frequencies and the spring constant factors. As the spring constant factors increase, the fundamental frequencies of CNTRC beams rise linearly. This suggests that adjusting these parameters can effectively control and enhance the dynamic performance and stability of CNTRC beams supported by an elastic foundation.

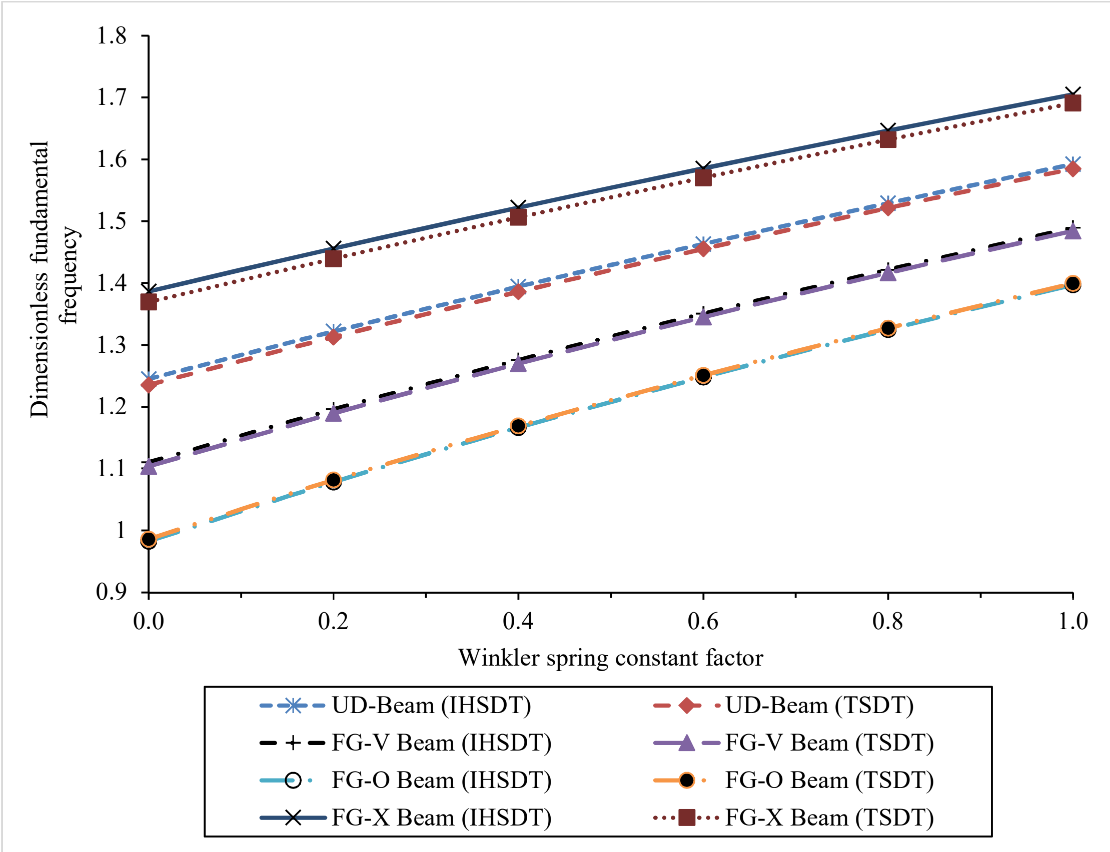

Figure 4.15. Effect of Winkler modulus parameter on the fundamental frequencies of CNTRC beams resting on a Pasternak elastic foundation with IHSDT and TSDT (*L/h* = 10; β_s= 0; V_{cnt}^* = 0.12)

4.5 Closure

This chapter presents comprehensive research on carbon nanotube reinforced composite beam structures. Solutions to various issues concerning carbon nanotube reinforced composite beam structures supported with and without elastic foundations have been identified, which will be beneficial for future studies. The effectiveness of the current trigonometric shear deformation theory, based on the secant function and inverse hyperbolic shear deformation theory, has been validated against several published beam models. The accuracy and efficacy of the current analytical formulations are demonstrated by comparing the results with established findings. The current solutions demonstrate effective static and dynamic responses for both carbon nanotube reinforced composite beam constructions, closely aligning with established results. The superior performance of the model compared to earlier approaches is attributed to two main factors: refinement of bending behavior using the secant function and inverse hyperbolic sine function, and satisfying the traction-free boundary conditions of transverse shear stresses.